Biogeochemical and Molecular Biological Characterization of Nitrogen Cycle Processes in the Columbia River and Estuary

By

Florian U. Moeller

A THESIS

Presented to the Division of Environmental and Biomolecular Systems

and the Oregon Health & Science University

in partial fulfillment of the requirements

for the degree of

Master of Science

in

Environmental Science and Engineering

January 2011

Division of Environmental and Biomolecular Systems

Institute of Environmental Health

Oregon Health & Science University

_____

CERTIFICATE OF APPROVAL

_____

This is to certify that the Master's thesis of

Florian U. Moeller

has been approved

_____
Dr. Joseph Needoba, Assistant Professor
Thesis Research Advisor

_____
Dr. Tawnya Peterson, Assistant Professor

_____
Dr. Holly M. Simon, Assistant Professor

_____
Dr. Peter Bottomley, Oregon State University
External Examiner

TABLE OF CONTENTS

LIST OF TABLES

LIST OF FIGURES

ACKNOWLEDGEMENTS

First and foremost, I would like to thank my thesis advisor, Dr. Joseph A. Needoba, whose confidence, support, and creativity provided a stable foundation and a clear path for the completion of this Master's thesis. It was a pleasure to have had the experience of interacting with a research mentor as operationally and intellectually accessible. These were all qualities and conditions which contributed extensively to my personal and intellectual growth.

Additionally, I would like to thank my examination committee members, Drs. Tawnya A. Peterson, Holly M. Simon, and Peter J. Bottomley, for taking the time to review and comment on this thesis. In particular, I would like to thank Dr. Peterson for her help with some of the statistical analyses included in this thesis and Dr. Simon for giving me access to her expertise, her laboratory as well as the expertise of her graduate students, Mou-zhong Xu and Christina Brow, who were indispensable in their help. Also, I would like to thank our collaborators at the University of Washington – Seattle, especially Dr. Willm Martens-Habbena, whose creative zeal kept me going near the end of my experiments.

Finally, I am profoundly grateful to the years of unwavering emotional and financial support from my family and friends. Special shout-outs go to my grandmother, who passed away during the completion of this thesis, and to my fiancée, Natasha Rivera, for her calming influence during the most stressful times of research and writing.

ABSTRACT

Biogeochemical and Molecular Biological Characterization of Nitrogen Cycle Processes in the Columbia River and Estuary

Florian Unschang Moeller, B.S.

M.S., Environmental Science and Engineering

at Oregon Health & Science University

January 2011

Supervising Professor: Dr. Joseph A. Needoba

Human induced changes in the nitrogen cycle on land are recorded in the nitrogen flux of rivers, which integrate the landscape processes in their watersheds and deliver materials to coastal systems. The annual global creation of fixed reactive nitrogen (Nr) from human activities is greater than 50% of naturally fixed Nr. As a result, the flux of Nr to aquatic habitats and the subsequent eutrophication of estuarine and coastal ecosystems has become a major environmental health issue. In addition, Nr is a source of the potent greenhouse gas, N_2O and may be tightly linked to the global carbon cycle, thus potentially affecting global CO_2 levels. Quantifying the increased Nr flux is difficult

since multiple contributing factors occur at different scales and interact to produce rapid and sometimes unpredictable changes in the biogeochemical cycle of Nr. The microbially-mediated processes of nitrification and denitrification are tightly linked and govern the recycling and removal processes, respectively, in the global Nr cycle. They are processes that also occur at different spatial and hence, temporal scales. This thesis is an assessment of the role of nitrification in Nr cycling in the Columbia River System (CRS), which includes its plume, estuarine mixing zone, and fluvial reaches. As the Columbia River is the largest source of freshwater entering the eastern boundary of the North Pacific Ocean it can exert a major influence on regional biogeochemical processes. Chapter 1 provides an introduction to the biogeochemical reactions in the Nr cycle. Chapter 2 describes an improved adaptation of the methodology for the fluorometric determination of ammonium that corrects for the absorptive interferences of dissolved organic carbon (DOC). Chapter 3 is a spatial and temporal study of nitrification carried out in the CRS, using molecular biological characterization, chemical sensor time series, ^{15}N natural abundance stable isotope time series, and ^{15}N stable isotope tracer experiments. The primary results of this research are that ammonia-oxidizing archaea (AOA) may be significant contributors to the first and rate-limiting step of nitrification, ammonia oxidation, in salinity-influenced stretches of the Columbia River estuary during upwelling events as well as during low flow, low nutrient conditions in the Columbia River, thereby highlighting the spatial and temporal sensitivity of these processes.

CHAPTER 1

Introduction

1.1 The Importance of Anthropogenic Nr

Nitrogen is essential to life on Earth, as it is a crucial building block of both amino acids and nucleic acids. Although it is most abundant in the Earth's atmosphere as triple-bonded nitrogen gas (N_2), where it constitutes 80% of its total mass (Galloway and Cowling, 2002), this enormous pool of N is not biologically available except to certain microorganisms which possess specialized metabolic machinery capable of fixing N_2 into active reduced forms such as ammonia (NH_3), amines and amino acids (Cowling and Galloway, 2002). In an oxygenated environment, reactive oxidized forms of N (Nr; e.g. NO_2^-, NO_3^-, NO_x, and N_2O) can then materialize and circulate in the atmosphere and biosphere as a result of a variety of abiotic and biotic reactions. In the pre-industrial world, biological nitrogen fixation was the dominant mode by which new reactive nitrogen (Nr) was made available to living organisms (Galloway and Cowling, 2002).

The fundamental necessity of N to all life was not discovered until the mid-19th century, which eventually led to the invention, in 1913, of the Haber-Bosch process, a chemical process to convert atmospheric N_2 to NH_3, and hitherto allowed a nearly unlimited supply of nitrogen that could be used to grow food. The newfound capacity for

food production was an important factor in the unprecedented rise in global human population during the 20th century and contributed, along with deforestation, increased legume and rice production, and emissions of NO_x from fossil fuel combustion, to a substantial and proportional increase in anthropogenically derived reactive nitrogen to the atmosphere and biosphere. Anthropogenic contributions to the global Nr pool grew from approximately 15 Tg N yr^{-1} in 1890 to 187 Tg N yr^{-1} in 2005, while during the same time naturally fixed reactive N actually decreased from ~245 Tg N yr^{-1} to ~234 Tg N yr^{-1} (Galloway and Cowling, 2002). A variety of positive and negative effects of a global increase in Nr have been documented, with these effects proceeding in a sequential nature through different environmental compartments and processes known as the nitrogen cascade (Galloway, 1998; Galloway *et al.*, 2003). Notable direct effects of this nitrogen cascade include the well documented cases of coastal eutrophication (Rabalais, 2002), the potential to significantly affect the global carbon cycle due to its tight linkage to the global nitrogen cycle (Gruber and Galloway, 2008), and the concurrent increase in the potent greenhouse gas, N_2O. All three of these processes can occur in aquatic systems where a substantial portion of Nr is transferred as part of the N cascade.

In the case of Nr in aquatic systems, nitrate (NO_3^-) and ammonium (NH_4^+) are the most abundant inorganic forms. Biological reactions dominate the production and removal mechanisms of these chemical species, although physicochemical conditions can determine the mobility and reaction conditions. Ammonium is typically a product of microbial organic matter remineralization or direct excretion by animals and fish. In aqueous solution, ammonium and un-ionized ammonia form a pH dependent equilibrium according to the relationship $NH_3 + H_2O \leftrightarrow NH_4^+ + OH^-$, such that at values lower than

approximately pH-9, ammonium concentrations are proportionally higher and vice versa. Ammonia can be biologically oxidized into nitrite (NO_2^-), by two groups of chemolithoautotrophic microorganisms, ammonia oxidizing bacteria (AOB) and ammonia oxidizing archaea (AOA). Nitrite can then be biologically oxidized to nitrate by one group of chemolithotrophic bacteria. This two-step process, called nitrification, occurs ubiquitously in oxygenated environments and is primarily responsible for the large deep ocean nitrate reservoir. In anoxic environments, denitrification can occur: 1) in a process known as 'anammox', whereby ammonium is biologically oxidized using nitrite as a terminal electron acceptor in a chemolithotrophic process to produce N_2 gas or, 2) through canonical denitrification, whereby nitrate is reduced to N_2 through a series of intermediate gaseous nitrogen oxide products which are all used as terminal electron acceptors in the oxidation of organic matter. Ammonium and nitrate are essential nutrients for primary producers, with ammonium being the most energetically favorable for growth (Owens and Esaias, 1976). These consumption processes, however still keep nitrogen in the reactive nitrogen pool. Therefore, the only permanent removal to N_2 is by denitrification, which is frequently coupled to nitrification as the biogeochemical pathway that creates nitrate. In addition, inefficiencies in these two central processes of the global nitrogen cycle are the primary determinants of atmospheric N_2O concentrations.

As of 1997, 60 percent of the world's population lived within 100 km from the coast (Cohen et al., 1997), with this coastal 100 km strip representing 18.7% of the total land area (Dao, 1998) and thus making the average human population density in coastal areas to be about twice the global average at around 80 persons/km^2. This figure is

skewed since many coastlines are sparsely populated or uninhabited, and yet it is

increasing yearly with about 50 million more people moving into the coastal zone

worldwide annually (CIESIN *et al.*, 2000). Furthermore, rivers can deliver more Nr from

inland sources and population centers to the coastal zone, with a significant amount of

anthropogenic nitrogen delivered to the coastal ocean thorough rivers (Gruber and

Galloway, 2008). Primary production in most coastal rivers, bays, and seas is limited by

nitrogen supply, and thus increased Nr inputs promote a progression of symptoms, known

as eutrophication, which begin with excessive growth of phytoplankton and macroalgae

to the point where grazers cannot control growth. Effects of this excessive growth include

anoxia or hypoxia in stratified waters, loss of submerged aquatic vegetation due to

increased shading, and decreases in benthic and phytoplankton diversity that can manifest

in nuisance/toxic algal blooms (Vitousek *et al.*, 1997).

Eutrophication of estuaries and coastal seas perhaps represents the greatest threat

to the integrity of coastal ecosystems and in the United States roughly 64% of assessed

estuaries had a moderate high or high overall eutrophic condition (OEC; Bricker *et al.*,

2007). Notably, the Pacific Coast region only had 19% of assessed estuaries with a

moderate high or high overall eutrophic condition. This result is partially a result of the

high flushing rates and dilution capabilities of estuaries in the northern Pacific region.

Nevertheless, 18 out of the 39 total estuaries on the Pacific Coast, including the Columbia

River Estuary, were not assessed, due to a dearth of data and poor or nonexistent

quantification of nitrogen loading data. Also, the amount of rainfall and the ratio of

watershed area to estuarine area, both of which can be significant factors in determining

the development of eutrophication, are some of the highest in the northern Pacific Coast region (Bricker *et al*. 2007).

1.2 The Columbia River System: physical, chemical, and biological complexity and its potential effects on Nr

The Columbia River System (CRS) stands out conspicuously in the Pacific Northwest as it is the second largest river in the United States with a drainage basin of 660,480 km^2 (van der Leeden *et al*., 1990) and is the largest source of freshwater to the northeastern Pacific Ocean (Simenstad *et al*., 1990). Moreover, the Columbia River (CR) watershed has the 5th densest watershed population in the U.S., including areas of intense agricultural activity, namely in the Willamette River and Yakima River tributary valleys. In Bricker *et al*. (2007), the Columbia River Estuary (CRE) was described to be not especially susceptible to eutrophication primarily due to its high flushing rate but was not given an OEC, chiefly due to a lack of nitrogen load data. Furthermore, Nr flux to the northeastern Pacific Ocean derived from the Columbia River Plume (CRP) may fuel particulate organic carbon (POC) export to the deep ocean and serve to decrease atmospheric CO_2 levels (Hales *et al*., 2006). This is in contrast to upwelled Nr (typically NO_3^-) which fuels POC export but has no net effect on atmospheric CO_2 (Sarmiento and Gruber, 2006), although Hales *et al*., (2006) did postulate a mechanism for transport of upwelling-derived POC from the continental shelf to the deep ocean. The need for improved monitoring of Nr flux in the Columbia River System, with its potential effects on coastal eutrophication and POC export to the deep ocean, is clear.

The remineralization, mobilization, and removal of Nr in upland systems prior to its delivery to the coastal ocean are significant processes to account for when determining Nr flux to coastal systems. Nitrification produces nitrate, which is highly soluble compared to the remineralized ammonium substrate, and thus increases Nr mobility in the hydrological cycle. When this process occurs in soils, the nitrate produced can be easily leached and advected via terrestrial runoff (Chester, 2003) or denitrified in soils. Globally, soil denitrification removes 46% of newly fixed terrestrial Nr, while river denitrification removes only 13% (Seitzinger et al., 2006). The presence of red alder, which have symbiotic N_2 fixers associated with their roots and occur exclusively in the North American Pacific Northwest, has been shown to substantially increase nitrate concentrations in nearby watersheds of the Oregon Coast Range (Compton *et al.*, 2003). Their presence in conifer-dominated soil ecosystems have also been associated with increased gross and net nitrification potentials (Boyle *et al.*, 2008; Boyle-Yarwood *et al.*, 2008) while denitrification has been found to be negligible in alder-conifer as well as conifer-only stands (Binkley *et al.*, 1992). The overall quantitative contributions of nitrification and denitrification to Nr export in the Columbia River basin are however unclear.

Since water residence time is an important determinant of denitrification (Seitzinger *et al.*, 2006), the high flow rate of the Columbia River would suggest a low denitrification potential. However, the Columbia-Snake River system is currently highly flow-regulated due to the imposition of fourteen major hydroelectric dams during the early to mid-20th century, which has considerably reduced the peak seasonal discharge – by 30% from ~ 17,500 m^3/s before extensive regulation to ~ 12,000 m^3/s at present

(Sherwood *et al.*, 1990) – but not the mean annual discharge (~ 7,300 m^3/s; Sherwood *et al.*, 1990; van der Leeden *et al.*, 1990). This set of significant engineering modifications should therefore promote denitrification, although recent studies indicate that increased nitrate uptake by phytoplankton and nitrification may have become more significant since river modification structures were installed (Sullivan *et al.*, 2001).

Prahl *et al*'s. (1998) survey of the lower Columbia River along with its tributary, the Willamette River, found a general downstream buildup of chlorophyll *a*, from the Bonneville Dam to the estuary, that was determined to be a recurring annual biological feature in the lower Columbia River in late spring to early summer (Bristow et al., 1985). This feature was deduced to be autochthonous, from Chl *a*:POC ratios, and did not display a concomitant drawdown of nutrients. They postulated that diffuse nutrient additions must have occurred in the lower Columbia River from agricultural runoff and other non-point source inputs, although the possibility of significant nutrient spiraling, including nitrification, was not included. Also, hyporheic flow paths, which can exchange a significant percentage of river flow and be areas of microbially mediated processes, were examined in off-channel alcoves in the Willamette River (Fernald *et al.*, 2006) and found to be potentially significant areas for nitrification, but not denitrification.

The CRE has a high flushing rate of 1 -3 d (Neal, 1972), which is primarily due to the high discharge of the Columbia River and the geomorphology of its estuary. It is narrow relative to its length, possesses few shallow, wide-mouthed bays and no substantial tributaries flow into its main channels (Prahl *et al.*, 1997). It is thus an area that is theoretically not a potentially significant contributor to denitrification and in fact, in Seitzinger *et al.*'s (2006) spatial analysis, the Columbia River was excluded since it

was considered to discharge directly to the continental shelf. By excluding rivers such as the Columbia, they estimated that estuarine denitrification accounts for the removal of only about 3% of newly fixed terrestrial N, globally. Similarly, nitrification is also dependent on the residence time of a water body, since nitrite-oxidizing bacteria and ammonia oxidizing bacteria and archaea are characterized by slow growth rates (Gould and Lees, 1960; Boon and Laudelout, 1962; Keen and Prosser, 1987; Konneke et al., 2005).

The CRE does, however, exhibit well-characterized estuarine turbidity maxima (ETM) that promote trapping and increased residence time of organic and inorganic particulate matter within the CRE (Jay *et al*., 1990; Reed and Donovan, 1994). These transient, sedimentary features are thus areas of elevated and particle-associated heterotrophic activity, with the CRE being a prime example (Baross *et al*., 1994; Crump and Baross, 1996). Since suspended particles have been shown to be positively correlated to potential nitrification rates in estuaries (Brion *et al*., 2000) and rivers (Xia *et al*., 2009), ETMs are also areas expected to exhibit enhanced nitrification activity, as found for example, in the Tamar estuary (Owens, 1986). Denitrification has been found to occur in the anoxic fluid mud layer of ETMs in the Gironde Estuary, although, since the conditions required for this process to happen are highly specific and transient, denitrification was not determined to be significant (Abril *et al*., 2000).

Salinity is another important factor controlling primary productivity, nitrification rates and ammonia-oxidizer communities. Based on a recurring seasonal pattern of phytoplanktonic POC transport from the CR to the mouth of the CRE, Lara-Lara *et al*. (1990) suggested that freshwater phytoplankton cells lyse and sink out of surface waters

upon exposure to salinities of ~2 – 5 psu, thereby contributing to a POC-rich ETM

particle load. Salinity has been observed to decrease nitrification (Rysgaard *et al.*, 1999;

Brion *et al.*, 2000; Cébron *et al.*, 2003), as well as denitrification rates (Rysgaard *et al.*,

1999). However, some studies have observed increased or similar nitrification rates

relative to freshwater rates at intermediate salinities (Berounsky and Nixon, 1993) or in

ETMs (Owens, 1986), which typically form at intermediate salinities. Decreases in

nitrification with increasing salinity have been explained by proportional NH_4^+ efflux,

from negatively charged binding sites within sediments, as salinity increases (Boatman

and Murray, 1982; Boynton and Kemp, 1985). On the other hand, salinity has been

shown to affect nitrifier species composition (de Bie *et al.*, 2001; Bollmann and

Laanbroek, 2002) as well as the relative abundances of AOA to AOB (Bernhard and

Bollmann, 2010 and references therein). These relationships are far from robust, but do

suggest a linkage between ammonium availability as dictated by physico-chemical

interactions and the nitrifier community responses to them.

1.3 Rationale

The magnitude of Nr flux from watersheds and the subsequent transformations in rivers

and estuaries is still relatively uncertain despite decades of monitoring. Most monitoring

programs rely on monthly or weekly samples, which undersample many water quality

variations (Johnson *et al.*, 2007). Also, most historical nitrogen measurements quantified

nitrate but did not measure ammonium. Notably, the chemical measurement of

ammonium has been fraught with uncertainty and inconsistency (Aminot *et al.*, 1997).

The recently and widely adopted fluorometric method for the determination of ammonium (Holmes *et al*., 1999) is highly sensitive and accurate, but suffers potential matrix effects from high dissolved organic carbon (DOC) concentrations. High DOC concentrations are frequently seen in major rivers of the world, particularly during high discharge periods.

Meanwhile, studies in the CRS have typically occurred in the summer when river flow is at its lowest and have found low river or high upwelled nitrate concentrations that seem to behave conservatively in the CRE (Bruland *et al*., 2008). This conservative behavior may simply reflect the low rates of nitrate uptake and production within the estuary due to short residence times, salinity effects, and dominance of heterotrophic activities. On the other hand, a balance between nitrate transformations by phytoplankton and denitrifiers with nitrate addition by nitrifiers is also possible. Annual studies have determined that nitrate concentrations in the CR are at a maximum in winter and early spring (>20 μM) coincident with high winter rainfall and spring snowmelt respectively (Lara-lara *et al*., 1990). In their analysis of Oregon Coast Range riverine nutrient inputs, Wetz *et al*. (2006) speculated that the supply of nutrients peaking in the winter may supply a significant proportion of carbon fixation as compared to summer upwelling derived carbon fixation. It is therefore unclear what the fate of Nr is during these periods of high Nr delivery from the lower Columbia River.

The proportion of AOA to AOB and their contributions to ammonia oxidation, in estuarine and riverine systems is still under investigation, since only a small number of comparable studies are available. AOA:AOB ratios have been found to generally decrease with increasing salinity in a subterranean estuary (Santoro *et al*., 2008),

estuarine sediments (Mosier and Francis, 2008; Bernhard *et al*., 2010), and salt marsh sediments (Moin *et al*., 2009). Since most oceanic studies exhibit AOA numerical dominance over AOB, often by orders of magnitude, one would expect increasing AOA:AOB ratios with increasing salinity. Indeed, Caffrey *et al*. (2007) found a significant positive correlation between AOA and salinity, across all 6 estuaries studied. Only one study has examined the relative abundance of AOA to AOB in a river (Liu *et al*., 2010), with AOA dominance determined in all examined samples.

1.4 Objective

The work presented here is an assessment of Nr cycling in the CRS using chemical sensor, fluorometric, isotopic and molecular biological techniques. Chapter 2 outlines an improvement on the fluorometric method for the measurement of ammonium in natural waters (Kérouel and Aminot, 1997; Holmes *et al*., 1999), using fluorescence spectroscopy to reduce the inner filter effects (IFE) of dissolved organic carbon (DOC), which can reach high concentrations in major rivers and other freshwater bodies of the world. Chapter 3 comprises a spatial and temporary survey of nitrification in the CRS, using molecular characterization of populations of AOA and AOB, along with chemical sensor time series, ^{15}N natural abundance stable isotope time series and ^{15}N stable isotope tracer rate experiments. Additionally, with the chemical sensor time series data, high resolution Nr net flux calculations from the lower Columbia River to the CRE are now possible. Finally, Chapter 4 presents a synthesis of these individual studies as they relate

to improving our knowledge and determining future areas of interest regarding Nr cycling in the CRS.

1.5 References

Abril, G., Riou, S. A., Etcheber, H., Frankignoulle, M., de Wit, R., and Middelburg, J. J. (2000). Transient, Tidal Time-scale, Nitrogen Transformations in an Estuarine Turbidity Maximum--Fluid Mud System (The Gironde, South-west France). *Estuarine, Coastal and Shelf Science* **50:** 703-715.

Aminot, A., Kirkwood, D. S., and Kérouel, R. (1997). Determination of ammonia in seawater by the indophenol-blue method: Evaluation of the ICES NUTS I/C 5 questionnaire. *Marine Chemistry* **56:** 59-75.

Baross, J.A., B. Crump, and C.A. Simenstad. (1994). Elevated 'microbial loop' activities in the Columbia River estuarine turbidity maximum. In *Changes in fluxes in estuaries: Implications from science to management*, ed. K.R. Dyer and R.J. Orth, 459–464. Fredensborg: Olsen & Olsen.

Bernhard, A. E., and Bollmann, A. (2010). Estuarine nitrifiers: New players, patterns and processes. *Estuarine, Coastal and Shelf Science* **88:** 1-11.

Bernhard, A. E., Landry, Z. C., Blevins, A., de la Torre, J. R., Giblin, A. E., and Stahl, D. A. (2010). Abundance of Ammonia-Oxidizing Archaea and Bacteria along an Estuarine Salinity Gradient in Relation to Potential Nitrification Rates. *Appl Environ Microbiol* **76:** 1285-1289.

Berounsky, V. M., and Nixon, S. W. (1993). Rates of Nitrification along an Estuarine

Gradient in Narragansett Bay. *Estuaries* **16:** 718-730.

de Bie, M. J. M., Speksnijder, A. G. C. L., Kowalchuk, G. A., Schuurman, T., Zwart, G.,
Stephen, J. R., Diekmann, O. E., and Laanbroek, H.J. (2001). Shifts in the
dominant populations of ammonia- oxidizing b-subclass Proteobacteria along the
eutrophic Schelde estuary. *Aquatic Microbial Ecology* **23:** 225-236.

Binkley, D., Sollins, P., Bell, R., Don Sachs, and Myrold, D. (1992). Biogeochemistry of
Adjacent Conifer and Alder-Conifer Stands. *Ecology* **73:** 2022-2033.

Boatman, C. D., and Murray, J. W. (1982). Modeling Exchangeable NH4 + Adsorption in
Marine Sediments: Process and Controls of Adsorption. *Limnology and
Oceanography* **27:** 99-110.

Bollmann, A., Bar-Gilissen, M., and Laanbroek, H. J. (2002). Growth at Low
Ammonium Concentrations and Starvation Response as Potential Factors
Involved in Niche Differentiation among Ammonia-Oxidizing Bacteria. *Appl.
Environ. Microbiol.* **68:** 4751-4757.

Boon, B., and Laudelout, H. (1962). Kinetics of nitrite oxidation by Nitrobacter
winogradskyi. *Biochemical Journal* **85:** 440-447.

Boyle, S. A., Yarwood, R. R., Bottomley, P. J., and Myrold, D. D. (2008). Bacterial and
fungal contributions to soil nitrogen cycling under Douglas fir and red alder at
two sites in Oregon. *Soil Biology and Biochemistry* **40:** 443-451.

Boyle-Yarwood, S. A., Bottomley, P. J., and Myrold, D. D. (2008). Community
composition of ammonia-oxidizing bacteria and archaea in soils under stands of
red alder and Douglas fir in Oregon. *Environmental Microbiology* **10:** 2956-2965.

Boynton, W.R.*,* and Kemp, W.M. *(*1985*)* Nutrient regeneration and oxygen-consumption

by sediments along an estuarine salinity gradient. *Mar Ecol Prog Ser* **23***:* 45–55.

Bricker, S.B*.,* Clement, C.G*.,* Pirhalla, D.E*.,* Orlando, S.P*.,* and Farrow, D.R.G. *(*2007*)*
National Estuarine Eutrophication Assessment: Effects of Nutrient Enrichment in
the Nation's Estuaries. Silver Spring, MD, USA: NOAA, National Ocean Service.
Special Projects Office and the National. Centers for Coastal Ocean Science.

Brion, N., Billen, G., Guézennec, L., and Ficht, A. (2000). Distribution of Nitrifying
Activity in the Seine River (France) from Paris to the Estuary. *Estuaries* **23:** 669-
682.

Bristow, M. P. F., Bundy, D. H., Edmonds, C. M., Ponto, P. E., Frey, B. E., and Small, L.
F. (1985). Airborne laser fluorosensor survey of the Columbia and Snake rivers:
simultaneous measurements of chlorophyll, dissolved organics and optical
attenuation. *International Journal of Remote Sensing* **6:** 1707-1734.

Bruland, K. W., Lohan, M. C., Aguilar-Islas, A. M., Smith, G. J., Sohst, B., and Baptista,
A. (2008). Factors influencing the chemistry of the near-field Columbia River
plume: Nitrate, silicic acid, dissolved Fe, and dissolved Mn. *Journal of*
Geophysical Research (Oceans) **113**.

Caffrey, J. M., Bano, N., Kalanetra, K., and Hollibaugh, J. T. (2007). Ammonia oxidation
and ammonia-oxidizing bacteria and archaea from estuaries with differing
histories of hypoxia. *The ISME Journal* **1:** 660-662.

Cébron, A., Berthe, T., and Garnier, J. (2003). Nitrification and Nitrifying Bacteria in the
Lower Seine River and Estuary (France). *Applied and Environmental*
Microbiology **69:** 7091-7100.

Chester, R. (2003). *Marine geochemistry*. Wiley-Blackwell.

CIESIN, IFPRI, WRI (2000). Gridded Population of the World (GPW), Version 2. Center
for International Earth Science Information Network (CIESIN), International
Food Policy Research Institute (IFPRI), World Resources Institute (WRI),
http://sedac.ciesin.columbia.edu/plue/gpw.

Cohen, J. E., Small, C., Mellinger, A., Gallup, J., Sachs, J., Vitousek, P. M., and Mooney,
H. A. (1997). Estimates of Coastal Populations. *Science* **278:** 1209.

Compton, J. E., Church, M. R., Larned, S. T., and Hogsett, W. E. (2003). Nitrogen
Export from Forested Watersheds in the Oregon Coast Range: The Role of N 2 -
fixing Red Alder. *Ecosystem* **6:** 773-785.

Cowling, E. B., and Galloway, J. N. (2002). Challenges and opportunities facing animal
agriculture: Optimizing nitrogen management in the atmosphere and biosphere of
the Earth. *J. Anim Sci.* **80:** E157-167.

Crump,B.C., and Baross, J.A. (1996). Particle-attached bacteria and heterotrophic
plankton associated with the Columbia River estuarine turbidity maxima. *Marine
Ecology Progress Series* **138:** 265-273.

Dao, Hy. 1998. Calculated for Earthwatch by Hy Dao, Department of Geography,
University of Geneva, using ArcWorld (1:3,000,000) with horizontal distances
corrected for latitude.

Fernald, A. G., Landers, D. H., and Wigington, P. J. (2006). Water quality changes in
hyporheic flow paths between a large gravel bed river and off-channel alcoves in
Oregon, USA. *River Research and Applications* **22:** 1111-1124.

Galloway, J. N. (1998). The global nitrogen cycle: changes and consequences.
Environmental Pollution **102:** 15-24.

Galloway, J. N., and Cowling, E. B. (2002). Reactive Nitrogen and the World: 200 Years of Change. *Ambio* **31:** 64-71.

Gould, G. W., and Lees, H. (1960). The isolation and culture of the nitrifying organisms. Part I. Nitrobacter. *Canadian Journal of Microbiology* **6:** 299-307.

Gruber, N., and Galloway, J. N. (2008). An Earth-system perspective of the global nitrogen cycle. *Nature* **451:** 293-296

Hales, B., Karp-Boss, L., Perlin, A., and Wheeler, P. A. (2006). Oxygen production and carbon sequestration in an upwelling coastal margin. *Global Biogeochemical Cycles* **20**

Holmes, R. M., Aminot, A., Kérouel, R., Hooker, B. A., and Peterson, B. J. (1999). A simple and precise method for measuring ammonium in marine and freshwater ecosystems. *Canadian Journal of Fisheries and Aquatic Sciences* **56:** 1801-1808.

Galloway, J.N., Aber, J.D., Erisman, J.W., Seitzinger, S.P., Howarth, R.W., Cowling, E.B., and Cosby, B.J. (2003). The Nitrogen Cascade. *BioScience* **53:** 341-356.

Jay, D. A., Giese, B. S., and Sherwood, C. R. (1990). Energetics and sedimentary processes in the Columbia River Estuary. *Progress In Oceanography* **25:** 157-174.

Johnson, K. S., Needoba, J. A., Riser, S. C., and Showers, W. J. (2007). Chemical Sensor Networks for the Aquatic Environment. *Chemical Reviews* **107:** 623-640.

Keen, G., and Prosser, J. (1987). Interrelationship between pH and surface growth of Nitrobacter. *Soil Biology and Biochemistry* **19:** 665-672.

Kérouel, R., and Aminot, A. (1997). Fluorometric determination of ammonia in sea and estuarine waters by direct segmented flow analysis. *Marine Chemistry* **57:** 265-

275.

Konneke, M., Bernhard, A. E., de la Torre, J. R., Walker, C. B., Waterbury, J. B., and
Stahl, D. A. (2005). Isolation of an autotrophic ammonia-oxidizing marine
archaeon. *Nature* **437:** 543-546.

Lara-Lara, J. R., Frey, B. E., and Small, L. F. (1990). Primary Production in the
Columbia River Estuary. I. Spatial and Temporal Variability of Properties. *Pacific
Science* **44:** 17-37.

Leeden, F. V. D., Troise, F. L., and Todd, D. K. (1990). *The water encyclopedia*. CRC
Press.

Liu, Z., Huang, S., Sun, G., Xu, Z., and Xu, M. (2010). Diversity and abundance of
ammonia-oxidizing archaea in the Dongjiang River, China. *Microbiological
Research*.

Moin, N. S., Nelson, K. A., Bush, A., and Bernhard, A. E. (2009). Distribution and
Diversity of Archaeal and Bacterial Ammonia Oxidizers in Salt Marsh Sediments.
Appl Environ Microbiol **75:** 7461-7468.

Mosier, A. C., and Francis, C. A. (2008). Relative abundance and diversity of ammonia-
oxidizing archaea and bacteria in the San Francisco Bay estuary. *Environmental
Microbiology* **10:** 3002-3016.

Neal, V. T. (1972). Physical aspects of the Columbia River and its estuary, p. 19-40. *InA.
T. Pruter and D. L. Alverson (eds.), *The Columbia River Estuary and Adjacent
Coastal Waters*. University of Washington Press, Seattle, Washington.

Owens, O.H. and Esaias, W.E. (1976). Physiological Response of Phytoplankton to
Major Environmental Factors. *Ann. Rev. Plant. Physiol*. **27:** 461-483

Owens, N. (1986). Estuarine nitrification: A naturally occurring fluidized bed reaction? *Estuarine Coastal and Shelf Science* **22:** 31-44.

Prahl, F. G., Small, L. F., Sullivan, B. A., Cordell, J., Simenstad, C. A., Crump, B. C., and Baross, J. A. (n.d.). Biogeochemical gradients in the lower Columbia River. *Hydrobiologia* **361:** 37-52.

Prahl, F. G., Small, L. F., and Eversmeyer, B. (1997). Biogeochemical characterization of suspended particulate matter in the Columbia River estuary. *Marine Ecology Progress Series* **160:** 173-184.

Rabalais, N. N. (2002). Nitrogen in aquatic ecosystems. *Ambio* **31:** 102-112.

Reed, D. J., and Donovan, J. (1994). The character and composition of the Columbia River estuarine turbidity maximum, p. 445–450. *In* K. R. Dyer and R. J. Orth [eds.], *Changes in fluxes in estuaries: Implications from science to management*. Academic.

Rysgaard, S., Thastum, P., Dalsgaard, T., Christensen, P. B., and Sloth, N. P. (1999). Effects of Salinity on NH4+ Adsorption Capacity, Nitrification, and Denitrification in Danish Estuarine Sediments. *Estuaries* **22:** 21-30.

Santoro, A. E., Francis, C. A., de Sieyes, N. R., and Boehm, A. B. (2008). Shifts in the relative abundance of ammonia-oxidizing bacteria and archaea across physicochemical gradients in a subterranean estuary. *Environmental Microbiology* **10:** 1068-1079.

Sarmiento, J. L., and N. Gruber (2006), *Ocean Biogeochemical Dynamics* Princeton Univ. Press, Princeton, N. J.

Seitzinger, S., Harrison, J. A., Böhlke, J. K., Bouwman, A. F., Lowrance, R., Peterson,

B., Tobias, C., and Drecht, G.V. (2006). Denitrification across landscapes and
waterscapes: a synthesis. *Ecological Applications* **16:** 2064-2090.

Sherwood, C. R., Jay, D. A., Bradford Harvey, R., Hamilton, P., and Simenstad, C. A.
(1990). Historical changes in the Columbia River Estuary. *Progress In
Oceanography* **25:** 299-352.

Simenstad, C., Small, L., Davidmcintire, C., Jay, D., and Sherwood, C. (1990). Columbia
river estuary studies: An introduction to the estuary, a brief history, and prior
studies. *Progress in Oceanography* **25:** 1-13.

Sullivan, B. E., Prahl, F. G., Small, L. F., and Covert, P. A. (2001). Seasonality of
phytoplankton production in the Columbia River: A natural or anthropogenic
pattern? *Geochimica et Cosmochimica Acta* **65:** 1125-1139.

Vitousek, P. M., Aber, J. D., Howarth, R. W., Likens, G. E., Matson, P. A., Schindler, D.
W., Schlesinger, W. H., and Tilman, D.G. (1997). Technical Report: Human
Alteration of the Global Nitrogen Cycle: Sources and Consequences. *Ecological
Applications* **7:** 737-750.

Wetz, M. S., Hales, B., Chase, Z., Wheeler, P. A., and Whitney, M. M. (2006). Riverine
Input of Macronutrients, Iron, and Organic Matter to the Coastal Ocean off
Oregon, U.S.A., during the Winter. *Limnology and Oceanography* **51:** 2221-2231.

Xia, X., Yang, Z., and Zhang, X. (2009). Effect of suspended-sediment concentration on
nitrification in river water: importance of suspended sediment-water interface.
Environmental Science & Technology **43:** 3681-3687.

CHAPTER 2

Dissolved Organic Carbon Interferes with the Fluorometric Ammonium Assay via the Inner Filter Effect

2.1 Abstract:

The routine and accurate determination of ammonium concentrations is critical to our understanding of the nitrogen cycle in aquatic systems. Recently, a fluorometric method for the determination of ammonium, involving its reaction with orthophthaldialdehyde (OPA) and sulfite, has seen increasing use and widespread acceptance in a variety of applications and settings. However, interferences in sample matrices, known as matrix effects (ME), have been shown to have a considerable impact on the fluorometric ammonium assay, with dissolved organic carbon (DOC) isolated as a main contributor. In this work, we used spectrofluorometry and standard additions of ammonium added to different concentrations of DOC-amended deionized water, in order to elucidate the mechanisms of DOC interference with the fluorometric ammonium assay. We found that DOC interferes with the fluorometric ammonium assay, primarily via the inner filter effect (IFE). After absorbance correction, ME were reduced considerably but still

existent, pointing at additional and unresolved mechanisms of interference. Standard

addition curves of different concentrations of DOC-amended DI water became more

similar after application of the IFE correction, and indicate that without it, the standard

additions method would overestimate ammonium concentrations. The IFE correction as

applied to the fluorometric ammonium assay is highly relevant in systems with variable

and high concentrations of DOC, and allows for the possibility for the use of one standard

additions curve for a large set of samples – thereby reducing reagent use and analysis

time.

2.2 Introduction

Ammonium, along with nitrate, is one of the most abundant stable inorganic species of nitrogen and forms an important link in the nitrogen cycle in aquatic ecosystems. As a nitrogen source, ammonium is preferred over nitrate by autotrophs and heterotrophs (Kirchman, 1994; Wheeler & Kokkinakis, 1990), and can also determine niche partitioning in ammonia-oxidizing microorganisms (Martens-Habbena *et al*., 2009) and thus, nitrification rates. Ammonium is typically a product of atmospheric deposition, fertilizer application, microbial organic matter remineralization, direct excretion by animals, or dissimilatory nitrate reduction to ammonium (DNRA) (Kaspar *et al*., 1981;Christensen *et al*., 2000). Various human activities have, moreover, increased the global pool in natural waters causing well documented cases of eutrophication. Despite its relative abundance, ammonium concentrations in natural waters are normally in submicromolar concentrations, compounding the reality that measurements are highly prone to contamination and ammonium can be relatively unstable during sample preservation (Aminot *et al*., 1997).

The fluorometric method for the measurement of ammonium in natural waters, as developed by Kérouel and Aminot (1997) and Holmes et al. (1999), has gained widespread acceptance and increased use. The technique involves the reaction of ammonium with an orthophthaldialdehyde (OPA)-sulfite reagent to produce a highly fluorescent compound. The method is sensitive, has a low salt effect, uses non-toxic reagents and does not include dialysis (Aminot *et al*., 2001). Numerous automatic, manual, and *in situ* systems and protocols have adapted this method for fluorometric

ammonium determination in a variety of settings. The use of a single non-toxic working reagent makes it amenable to manual analyses in the field and in particular, to *in situ* sensor development. However, as noted by Holmes *et al*. (1999) and more recently by Taylor *et al*. (2007), matrix effects (ME) are important to account for in natural samples since the substances that cause ME can fluctuate through space and time in the environment.

ME for the fluorometric ammonium method have been studied to some extent. Potential interferences from salts and other ions such as bicarbonate and sulfide, as well as phytoplankton and particulate matter have shown minimal interferences (Aminot *et al*., 2001). Since OPA was first used in conjunction with thiols to detect amino acids (Roth, 1971), the ability of the OPA-sulfite complex to react with primary amines has also been studied, with mixed results (Genfa and Dasgupta, 1989; Amornthammarong and Zhang, 2008). Holmes *et al*. (1999) tested the ME associated with dissolved organic matter (DOM) and found increasing dissolved organic carbon (DOC) concentrations coincided with increased matrix effects. To account for these ME, Holmes *et al*. (1999) suggested spiking samples with a known amount of ammonium and comparing the response to the same amount added to standards. Taylor *et al*. (2007), however, pointed out that different concentrations of spikes yielded different ME and suggested using standard spike additions for each sample or set of similar samples for adequate accounting of ME in ammonium measurements. In addition, they focused their experiments by accounting for or manipulating the concentration of DOC, suggesting a role for it as a fluorescence quencher. Kang *et al*. (2003) have similarly found a decrease in the fluorescence intensity

of the OPA-sulfite-ammonium reaction with increasing DOC concentrations and attributed the decreases to quenching effects.

One ME on fluorescence measurements is the absorption properties of the sample, which can attenuate the incident and emitted light and are commonly known as primary and secondary inner filter effects (IFE), respectively (Lakowicz, 2006). Although IFEs are considered to be a fluorescence quenching mechanism in that they decrease the fluorescence intensity of a sample, they provide little information regarding molecular interactions and may distort more interesting quenching mechanisms. Nevertheless, the significance of IFEs is important to consider in any sample when analyzing fluorescence data. In studies characterizing DOM fluorescence spectra, IFE correction allows for the direct quantitative and qualitative comparison of samples with different DOC concentrations (Stedmon *et al*. 2003; McKnight *et al*., 2001) since increasing DOC concentrations in non-corrected samples have been shown to display a red shift in maximum excitation and emission fluorescence (Mobed *et al*., 1996).

In this work, we try to elucidate the mechanisms of DOC interference with the fluorometric ammonium assay by using fluorescence spectroscopy. This was done in combination with standard additions of ammonium to varying concentrations of DOC-amended DI water. An absorption correction was needed to account for the ME exerted by DOC. This study focuses on the differences in the standard addition curves and the ME before and after IFE correction, as well as the inferences we can make regarding other mechanisms of interference with respect to the fluorometric ammonium assay.

2.3 Materials and Methods

24

Standard additions of ammonium were added in the $0.25 - 5$ μM range to blank deionized (DI) water and varying concentrations of DOC amended DI water. Reagents and reaction conditions were similar to Holmes *et al.* (1999) and Taylor *et al.* (2007). Reactions were conducted in a 4:1 sample water to working reagent (WR) ratio as in Holmes *et al.*'s Protocol A (1999), although the volumes were reduced to 8 mL of sample water and 2 mL of WR. DOC amended water samples were prepared by dissolving natural organic matter (NOM) isolated from the Suwannee River (Serkiz and Perdue, 1990; International Humic Substances Society, http://www.ihss.gatech.edu) into DI water and calculating the DOC concentrations from the published carbon percentages in the NOM. A series of DOC amendment solutions with concentrations of 0, 6.25, 25, and 52.47 mg/L were prepared by serial dilution of a stock solution of 100 mg/L NOM.

A scanning fluorescence spectrophotometer (Fluoromax-4, Horiba Jobin-Yvon) was used to study potential interferences in the excitation and emission spectra between the DOC-WR product and NH_4^+-WR product. The generated excitation and emission spectra were used to verify the wavelengths that produced maximum emissions. Excitation scans used a bandwidth of $250 - 530$ nm and a slit width of 1 nm, while emission was measured at a bandwidth of $300 - 600$ nm and with a slit width of 1 nm, for the generation of the standard addition curves. For the generation of the excitation and emission spectra, excitation and emission scans used the same wavelength bandwidth but with slit widths of 5 and 2 nm respectively. An excitation wavelength of ~360 nm was verified to generate maximum emissions at ~422 nm. Fluorescence intensity was calibrated using the Raman scatter peak as suggested by Lawaetz and Stedmon (2009).

Finally, absorption for all samples was measured on a spectrophotometer (Titas-1, World

Precision Instruments) in a 1-cm quartz cuvette at wavelengths of 186 – 723 nm.

Fluorescence intensity was corrected for the inner filter effect (IFE) by using the

following equation (Lakowicz, 2006) :

$$F_{corr} = F_{obs}\, antilog\left(\frac{OD_{ex} + OD_{em}}{2}\right)$$

where F_{corr} is the fluorescence corrected for the IFE, F_{obs} is the uncorrected initial

fluorescence and OD_{ex} and OD_{em} are the optical density values at both the excitation and

emission wavelengths, respectively.

Standard addition curves were generated for F_{corr} and F_{obs} such that the

fluorescence of the standard additions is plotted against their nominal concentrations. The

concentration of contaminant ammonium and/or primary amines was ascertained by

determining the absolute value of the x-axis intercept of the linear regression of the

standard addition curves as in Taylor *et al.* (2007). Additionally, ME were determined for

each standard addition and DOC concentration. ME were calculated from Equation 3 in

Holmes *et al.* (1999) and averaged for each DOC concentration.

2.4 Results

2.4.1 *Excitation and emission spectra*

The excitation – emission spectra of both the OPA-sulfite-DOC and the OPA-sulfite-

NH_4^+ compounds (Figure 2.1a and 2.1b, respectively) indicate that maximum emissions

occurred at ~422 nm when the excitation wavelength was ~360 nm. Application of the

IFE correction results in the increase in fluorescence emissions for both compounds,

although the difference is more striking with the OPA-sulfite-DOC fluorogenic product.

Notably, for the OPA-sulfite-DOC compound, the maximum emissions consistently occurred at 422 and 424 nm at an excitation wavelength of 365 nm before the IFE correction and at an excitation wavelength of 360 nm after the IFE correction. On the other hand, the OPA-sulfite-NH_4^+ compound exhibited consistent excitation-emission maxima, at 360 and 422 nm respectively, before and after IFE corrections. Nonetheless, the excitation-emission spectra of both fluorogenic products are not drastically different, which points at the potential interference of primary amines or ammonia contamination, after the correction for DOC absorbance.

2.4.2 *Standard addition curves*

Initially, standard addition curves of DI water and DOC-amended DI water show that as DOC concentrations increased, the slopes of the curves decreased, indicating an additive interference effect for DOC (Figure 2.2a.). The interference is significant even at standard addition concentrations of 2.5 μM NH_4^+, and increased DOC concentrations resulted in very similar fluorescence values. Furthermore, at standard addition concentrations of 5.0 μM NH_4^+, the highest DOC concentrations have the lowest fluorescence values while the lowest DOC concentrations have the highest fluorescence values. After correction for the IFE, however, the slopes of the standard addition curves became more similar such that the curves were virtually parallel to each other (Figure 2.2b.). With the IFE correction, higher DOC and NH_4^+ concentrations resulted in consistently higher fluorescence values.

2.4.3 *Absorption spectra*

Examination of the absorption spectra of samples with only varying concentrations of DOC and without WR added (Figure 2.3) revealed that increasing concentrations of DOC caused a linear increase in absorption of the sample at the optimal excitation and emission wavelengths of the OPA-sulfite-NH_4^+ product . Most of the absorption affecting the fluorophore occurred at the optimal excitation wavelength of 360 nm. A slight but linear increase in absorption was also seen with increasing NH_4^+ in samples with only NH_4^+ and no WR added (data not shown). Additionally, the relationship between DOC concentration and the fluorescence intensity of the OPA-sulfite-DOC compound was linear (Figure 2.4).

2.4.4 *Primary amine concentrations and ammonium contaminants*

For the samples before the IFE correction, ammonium contaminant and/or primary amine concentrations as determined by the standard additions method for DOC concentrations of 0, 6.25, 25, and 52.47 mg/L were 0.15, 0.82, 2.54, and 5.03 μM respectively. For the samples after the IFE correction, ammonium contaminant and/or primary amine concentrations were 0.11, 0.75, 2.33, and 4.77 μM respectively. It is evident based on the blank DOC addition that a considerable amount of ammonium contamination occurred in the DI water sample, highlighting the need for fastidious user and method practices. More importantly, a consistent over-estimation of ammonium contamination and/or primary amines is apparent before application of the IFE correction.

2.4.5 *Matrix effects*

Increasing DOC concentrations resulted in higher ME, although after the IFE correction, the increase was smaller and less variable (Figure 2.5). The relationship between ME and DOC is statistically linear before the IFE correction ($R^2 = 0.9704$) and after the IFE correction ($R^2 = 0.9977$). However, after the IFE correction, the slope is significantly less steep and the points display overlapping standard deviations. Although the IFE correction removed considerable amounts of DOC-associated ME, DOC still exerts ME on the formation of the OPA-sulfite-NH_4^+ fluorogenic product.

2.5 Discussion

This work highlights the complex impact of DOC on the fluorometric ammonium assay, which is in itself a complex derivatization of a highly fluorescent isoindole and is limited in its mechanistic characterizations (Zuman, 2004). DOC is a heterogeneous mixture of organic compounds containing a nebulous combination of carboxyl, hydroxyl, and amine functional groups, and is well known for its ability to influence the transport processes and bioavailability of nutrients and contaminants. Since OPA is commonly used to detect primary amines and amino acids, DOC has the ability to form a fluorescent product while concurrently inhibiting fluorescence via a variety of possible processes such as quenching, complexation with the analyte, and the IFE. We were thus able to determine that DOC has a considerable IFE on the fluorometric ammonium assay and that after accounting for it, interferences were less variable and markedly reduced.

Following the IFE correction it is possible to use one standard addition slope for calculating ammonium values in a wider variety of samples via Protocol II as outlined in

Taylor *et al*. (2007). The protocol calls for the statistical determination of slope homogeneity among different sites and samples, after which a representative slope can be used to quantify subsequent ammonium concentrations based on each sample's fluorescence. The ability to achieve this is particularly relevant to instances where reagent and analysis time are limited, namely high resolution *in situ* spatial and temporal surveys. There have been several studies applying variations of the fluorometric ammonium assay to high-throughput flow-injection manifolds (Aminot *et al*., 2001; Amornthammarong and J. Zhang, 2008; Watson *et al*. 2005) and there are now several commercially available *in situ* nutrient analyzers that use the fluorometric method for ammonium determination.

A DOC concentration of 6.25 mg/L is sufficient to have a significant inner filter effect on OPA-sulfite-NH_4^+ fluorescence (Figure 2.4), with DOC concentrations of 25 and 52.47 mg/L having increasing and linear inner filter effects. Numerous major rivers in the world experience DOC concentrations spanning the 5-25 mg/L range, particularly during high discharge periods (Spitzy and Leenheer, 1991, Dissolved organic carbon in rivers. In: Degens et al. *SCOPE 42: Biogeochemistry of Major World Rivers*. Wiley, Chichester, pp 213–232). Furthermore, DOC concentrations in Blackwater rivers and wetlands can typically reach or exceed the maximum 52.47 mg/L value used in this study (Mann and Wetzel, 1995; Ma *et al*., 2001).

Without application of the IFE, the standard additions method of Taylor et al. (2007) would consistently overestimate ammonium concentrations in samples with high DOC concentrations. Moreover, as is apparent from the IFE-corrected standard additions curves as well as the excitation-emission spectra of the OPA-sulfite-DOM compound

30

(Figures 2.1 and 2.2), there is a measurable and identical signal produced by the DOM that can most likely be attributed to the interaction of the primary amines present in the DOM with OPA. Ammonium contamination from laboratory sources and methodology was around 0.10 μM. By assuming minimal ammonium contamination in the NOM isolation process and handling, the 6.25, 25, and 52.47 mg/L DOC samples are thus calculated to have primary amine contributions of 0.6, 2.2, and 4.7 μM. Based on the published nitrogen percentages in the Suwannee River NOM, we calculate the DOM-amended samples to have DON concentrations of 9.4, 37.4, and 78.6 μM respectively. As such, the fluorometric ammonium assay detects ~6% of the predicted DON concentration in the Suwannee River NOM.

Individual amino acid concentrations were not available for the Suwannee River NOM reference material, although amino acid concentrations are available for Suwannee River standard and reference humic and fulvic acid fractions (IHSS, http://www.ihss.gatech.edu). These materials are isolated from the same sample site as Suwannee River NOM and their composition is expected to be very similar but not identical. The sum of 7 quantified amino acids in both the humic and fulvic acid fractions, ranges from 7.8 - 8 μM in the 52.47 mg/L DOC-amended sample, and thus the published amino acid values contribute approximately 58 - 69% of the measured signal in all DOC-amended samples. Genfa and Dasgupta (1989), using the OPA-sulfite-NH_4^+ reaction, found that individual amino acids contributed between approximately 6 - 0.2 % of the measured signal compared to ammonium. By assuming the contribution of each amino acid is additive, the summed contribution of the 11 measured amino acids would

have been ~23%. Amornthammarong and Zhang (2008), using the same method and a different set of primary amines, found individual contributions between 123% and 64%

After accounting for the IFE, ME were still evident and exhibited a slightly linear increase with DOC concentration. Quenching mechanisms such as ground state complexation with the fluorophore, and static and collisional quenching, are all possible mechanisms. DOM and, specifically, humic acid complexations with ammonium are another well known set of mechanisms most likely contributing to the influence of DOC on the fluorometric ammonium assay. We think estuarine systems, preferably simulated, are model systems to study the effect of DOC on the OPA-sulfite-NH_4^+ reaction, as sea water has a desorptive impact on organic matter-NH_4^+ complexation (Boatman and Murray, 1982; Hou *et al*., 2003). In spite of the high sensitivity and general lack of interference effects of the current method, certain gaps in the mechanisms of this reaction exist, in particular with natural samples that do indeed affect the sensitivity of ammonium measurements. Future work on the theoretical and practical applications of the fluorometric ammonium method, are still needed.

2.6 Conclusions

- By using standard additions of ammonium to DI water with differing concentrations of DOC, we found that the fluorescence intensity generated from standard ammonium additions differed depending on the concentration of DOC. By applying the IFE correction we were able to generate standard curves that were more similar and less variable. Without application of the

IFE correction, the standard additions method would overestimate ammonium concentrations.

- Future applications of the fluorometric ammonium assay, especially in settings with variable and high concentrations of DOC, could apply the IFE correction such that one standard additions curve can be used with greater accuracy for a set of similar samples while concurrently reducing reagent use and analysis time.

- The use of standard additions of ammonium on DOC-amended DI water with the OPA-sulfite assay, allowed for the theoretical determination of DON and amino acid bulk contributions to the fluorogenic product. We found that the OPA-sulfite assay roughly detects ~6% and between 58-69% of DON and amino acid bulk concentrations, respectively, in Suwannee River NOM.

- Although the IFE correction significantly reduces apparent ME associated with high DOC concentrations, DOC still exerts some ME on the formation of the OPA-sulfite-NH_4^+ fluorogenic product. Mechanisms for this interaction should be further studied.

2.7 References

Aminot, A., Kirkwood, D.S. and Kérouel, R. (1997). Determination of ammonia in seawater by the indophenol-blue method: Evaluation of the ICES NUTS I/C 5 questionnaire. *Marine Chemistry* **56:** 59-75.

Aminot, A., Kérouel, R. and Birot, D. (2001). A flow injection-fluorometric method for the determination of ammonium in fresh and saline waters with a view to in situ analyses. *Water Research* **35:** 1777-1785.

Amornthammarong, N. and Zhang, J. (2008). Shipboard Fluorometric Flow Analyzer for High-Resolution Underway Measurement of Ammonium in Seawater. *Analytical Chemistry* **80:** 1019-1026.

Boatman, C.D. and Murray, J.W. (1982). Modeling Exchangeable NH4 + Adsorption in Marine Sediments: Process and Controls of Adsorption. *Limnology and Oceanography* **27:** 99-110.

Christensen, P.B., Rysgaard, S., Sloth, N.P., Dalsgaard, and T., Schwaerter, S. (2000). Sediment mineralization, nutrient fluxes, denitrification and dissimilatory nitrate reduction to ammonium in an estuarine fjord with sea cage trout farms. *Aquatic Microbial Ecology* **21:** 73-84.

Genfa, Z. and Dasgupta, P.K. (1989). Fluorometric measurement of aqueous ammonium ion in a flow injection system. *Analytical Chemistry* **61:** 408-412.

Holmes, R.M., Aminot, A., Kérouel, R., Hooker, B.A., and Peterson, B.J. (1999). A simple and precise method for measuring ammonium in marine and freshwater ecosystems. *Canadian Journal of Fisheries and Aquatic Sciences* **56:** 1801-1808.

Hou, L.J., Liu, M., Jiang, H.Y., Xu, S.Y., Ou, D.N., Liu, Q.M., and Zhang, B.L. (2003). Ammonium adsorption by tidal flat surface sediments from the Yangtze Estuary. *Environmental Geology* **45:** 72-78.

Kang, H., Stanley, E.H. and Park, S. (2003). A Sensitive Method for the Measurement of Ammonium in Soil Extract and Water. *Communications in Soil Science and Plant Analysis* **34:** 2193.

Kaspar, H.F., Tiedje, J.M. and Firestone, R.B. (1981). Denitrification and dissimilatory nitrate reduction to ammonium in digested sludge. *Canadian Journal of Microbiology* **27:** 878-885.

Kérouel, R. and Aminot, A. (1997). Fluorometric determination of ammonia in sea and estuarine waters by direct segmented flow analysis. *Marine Chemistry* **57:** 265-275.

Kirchman, D.L. (1994). The Uptake of Inorganic Nutrients by Heterotrophic Bacteria. *Microbial Ecology* **28:** 255-271.

Lakowicz, J.R., 2006. *Principles of fluorescence spectroscopy*, 3rd ed., Springer, New York.

Lawaetz, A.J. and Stedmon, C.A. (2009). Fluorescence intensity calibration using the Raman scatter peak of water. *Applied Spectroscopy* **63:** 936-940.

Ma, H., Allen, H.E. and Yin, Y. (2001). Characterization of isolated fractions of dissolved organic matter from natural waters and a wastewater effluent. *Water Research* **35:** 985-996.

Mann, C.J. and Wetzel, R.G. (1995). Dissolved organic carbon and its utilization in a riverine wetland ecosystem. *Biogeochemistry* **31:** 99-120.

35

Martens-Habbena, W., Berube, P.M., Urakawa, H., de la Torre, J.R., and Stahl, D.A. (2009). Ammonia oxidation kinetics determine niche separation of nitrifying Archaea and Bacteria. *Nature* **461:** 976-979.

McKnight, D.M., Boyer, E.W., Westerhoff, P.K., Doran, P.T., Kulbe, T., and Andersen, D.T. (2001). Spectrofluorometric Characterization of Dissolved Organic Matter for Indication of Precursor Organic Material and Aromaticity. *Limnology and Oceanography* **46:** 38-48.

Mobed, J.J., Hemmingsen, S.L., Autry, J.L., and McGown, L.B. (1996). Fluorescence Characterization of IHSS Humic Substances: Total Luminescence Spectra with Absorbance Correction. *Environmental Science & Technology* **30:** 3061-3065.

Roth, M. (1971). Fluorescence reaction for amino acids. *Analytical Chemistry* **43:** 880-882.

Serkiz, S.M. and Perdue, E. (1990). Isolation of dissolved organic matter from the Suwannee River using reverse osmosis. *Water Research* **24:** 911-916.

Spitzy, A., and Leenheer J. (1991). Dissolved organic carbon in rivers, p. 213-232. *In* Degens E.T., Kempe S., & Richey J.E. (ed.), *SCOPE 42: Biogeochemistry of Major World Rivers.* John Wiley and Sons Ltd., Chichester, United Kingdom.

Stedmon, C.A., Markager, S. and Bro, R. (2003). Tracing dissolved organic matter in aquatic environments using a new approach to fluorescence spectroscopy. *Marine Chemistry* **82:** 239–254.

Taylor, B.W., Keep, C.F., Hall, R.O., Koch, B.J., Tronstad, L.M., Flecker, A.S., and Useth, A.J. (2007). Improving the fluorometric ammonium method: matrix effects, background fluorescence, and standard additions. *Journal of the North*

American Benthological Society **26:** 167-177.

Watson, R.J., Butler, E.C., Clementson, L.A., and Berry, K.M. (2005). Flow-injection

analysis with fluorescence detection for the determination of trace levels of

ammonium in seawater. *Journal of Environmental Monitoring* **7:** 37-42.

Wheeler, P.A. and Kokkinakis, S.A. (1990). Ammonium Recycling Limits Nitrate Use in

the Oceanic Subarctic Pacific. *Limnology and Oceanography* **35**: 1267-1278.

Zuman, P. (2004). Reactions of Orthophthalaldehyde with Nucleophiles. *Chemical

Reviews* **104:** 3217-3238.

2.8 Figures
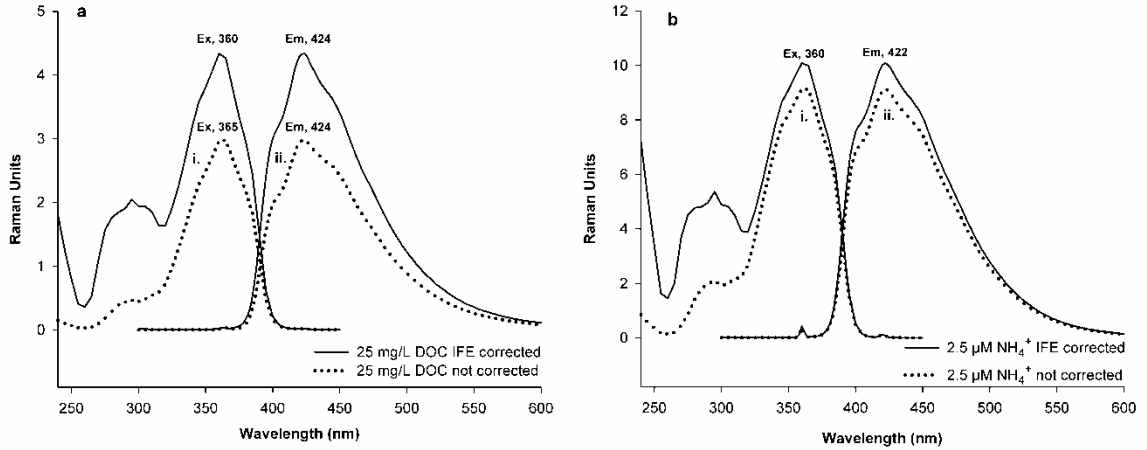
Figure 2.1 Excitation (i.) and emission (ii.) spectra for DI water amended with 25 mg/L DOC (a) and DI water amended with a 2.5 μM standard concentration of NH_4^+ (b) after incubation with WR for 2 h, before and after IFE correction
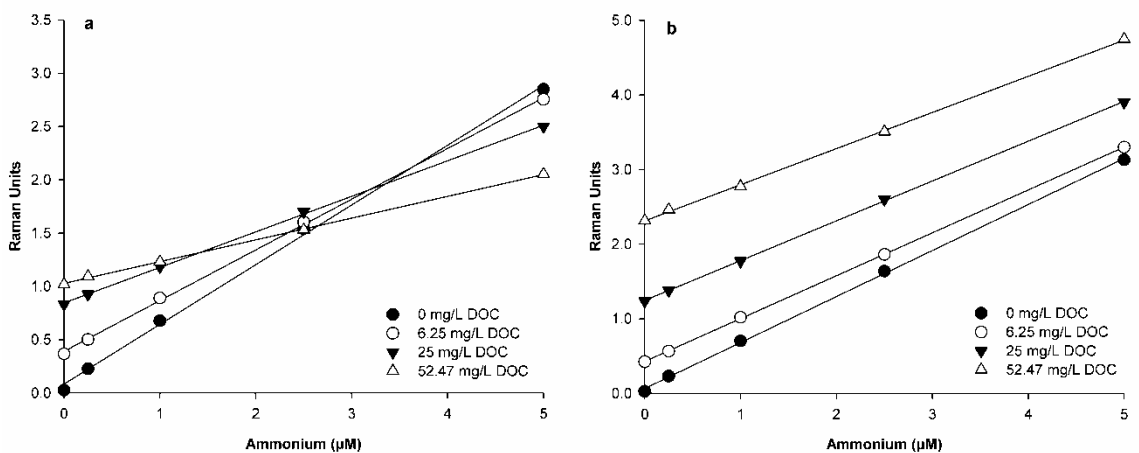
Figure 2.2 Standard addition curves of different concentrations of DOC-amended DI water, before (a) and after (b) the application of the inner filter effect.
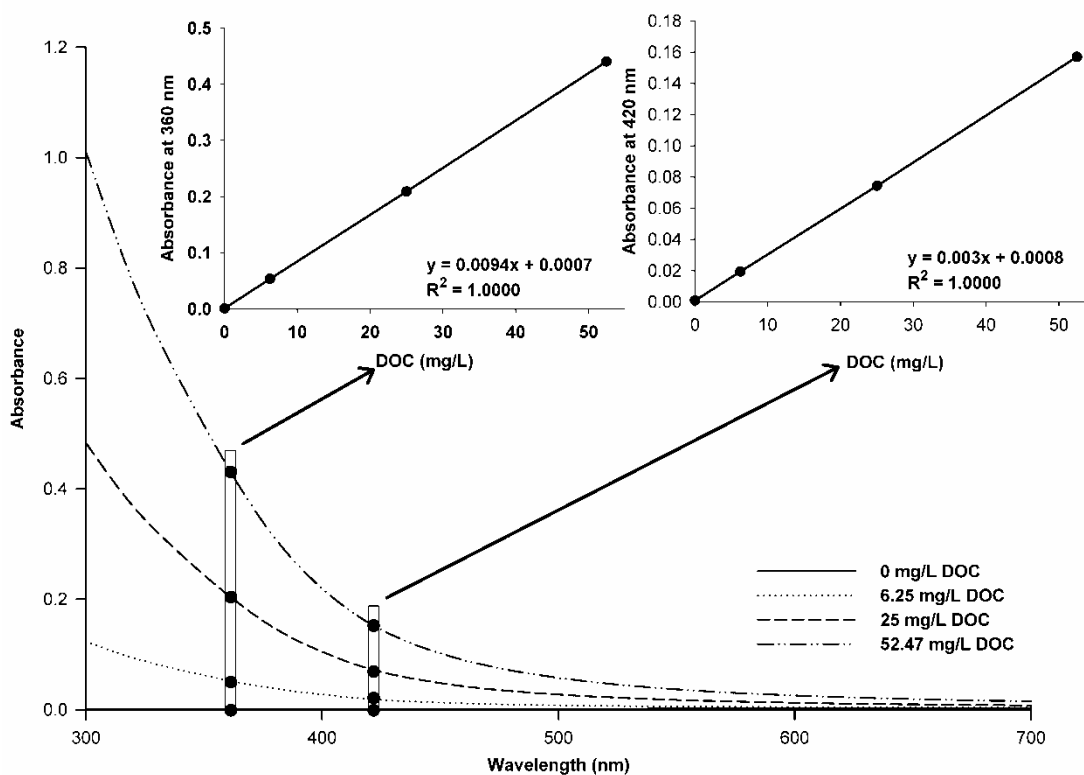
Figure 2.3 Absorption spectra of DOC-amended DI water. Insets depict the relationship between DOC concentrations in DI water and absorbance at the maximum excitation and emission wavelengths of the OPA-sulfite-NH_4^+ product, respectively.
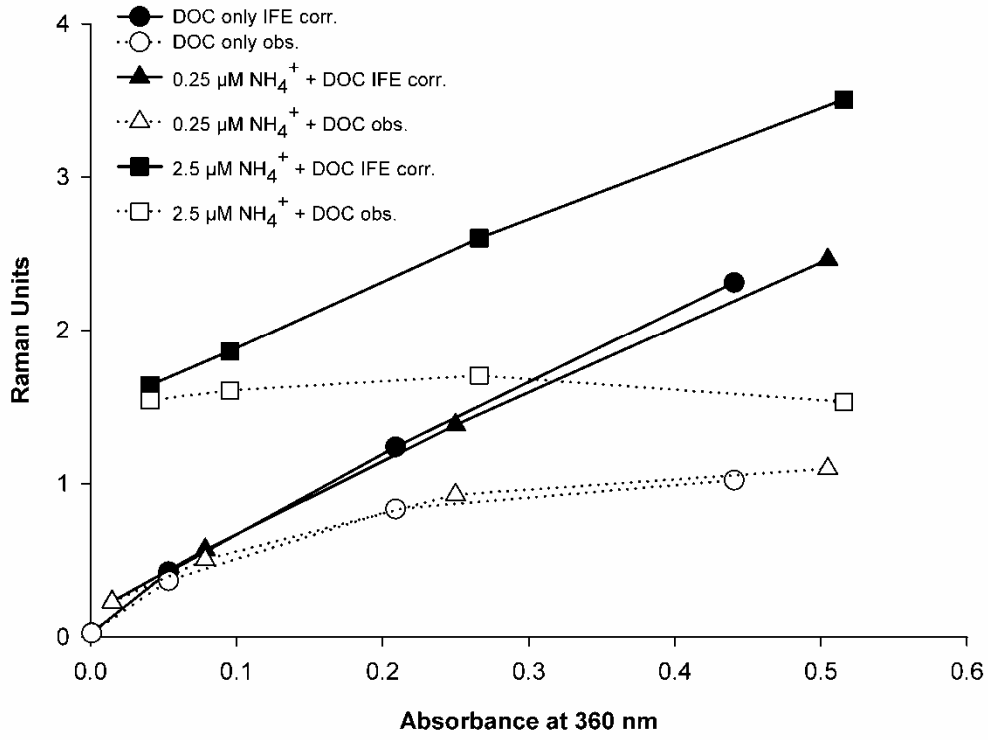
Figure 2.4 Effects of absorbance at 360 nm as caused by increases in DOC concentrations (0, 6.25, 25, and 52.47 mg/L DOC respectively) on the fluorescence intensity at ~422 nm of the OPA-sulfite-NH_4^+ product at different NH_4^+ concentrations.
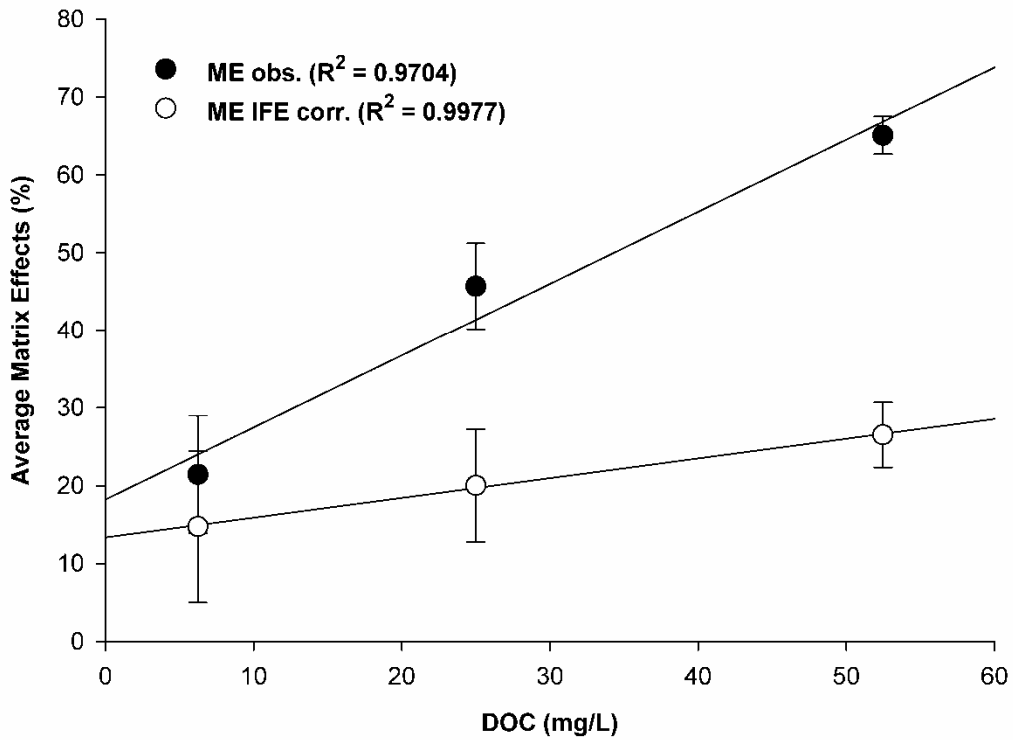
Figure 2.5 Quantification of average matrix effects (ME), expressed as percent reduction, from different spike concentrations at different concentrations of DOC in DI water before and after IFE correction.

CHAPTER 3

Molecular and Biogeochemical Characterization of Ammonia-oxidizing Archaea and Bacteria in the Lower Columbia River Estuary

3.1 Abstract

Ammonia-oxidation is the first and rate-limiting step in nitrification, a process that is critical to nitrogen cycling in estuarine and riverine environments. Ammonia-oxidation is believed to be dominated by two groups of microorganisms in most environments, the ammonia-oxidizing archaea (AOA) and the ammonia-oxidizing bacteria (AOB). Here we report a multiyear study of the relationships between the abundance of AOA, AOB in the β-proteobacterial subdivision (β-AOB), and environmental variables within the lower Columbia River Estuary – from the mouth of the Columbia River to the freshwater urban reaches near Portland, Oregon. In a spatial survey, AOA *amoA* gene abundance was found to be greater than β-AOB *amoA* gene abundance in most of the study area with the most pronounced differences associated with upwelled nutrient rich bottom waters in the estuary, contrasting reports where β-AOB from estuaries were more strongly associated with high salinity. Also, AOA *amoA* gene copies and the AOA:β-AOB *amoA* gene copy ratio were significantly correlated to ammonium and turbidity, respectively, indicating possible AOA niche partitioning, and particle attachment. Time series data showed a significantly negative correlation between the AOA:β-AOB *amoA* ratio and ammonium

and a significant positive correlation between β-AOB *amoA* and the magnitude of Willamette River discharge. Seasonally, the AOA:β-AOB *amoA* gene copy ratio was significantly and negatively correlated to nitrate and the $\delta^{15}N$ of nitrate ($r^2 = 0.849$, p < 0.01), suggesting that AOA were significant contributors to ammonia oxidation either *in situ* or as an integrative marker of runoff derived nitrification. Finally, nitrification rates were carried out using $^{15}NH_4^+$ and $^{15}NO_3^-$ tracer incubations, along with the nitrification inhibitor allylthiourea (ATU), in surface waters, and were found to mimic a coincident *in situ* nitrate increase. These results indicate that the observed nitrate increase in euphotic surface waters was most likely attributable mainly to AOA, a small proportion to β-AOB, and perhaps even heterotrophic nitrifiers.

3.2 Introduction

The creation of fixed reactive nitrogen (Nr – as defined by Galloway and Cowling, 2002) from N_2 by human activities has approximately doubled the annual rate of nitrogen input to the terrestrial nitrogen cycle since the pre-industrial era (Vitousek *et al.*, 1997). These changes in the nitrogen cycle influence the nitrogen flux of rivers, which drain their watersheds and transfer dissolved and particulate matter to estuaries and coastal oceans (Vitousek *et al.* 1997). As a result, the eutrophication of riverine, estuarine and coastal systems has become a major environmental and ecosystem health issue of a similar magnitude as global climate change induced by the perturbation of greenhouse gases. Nitrification, which is the sequential oxidation of ammonia to nitrite and then to nitrate, is a critical step in the nitrogen cycle and can mediate the removal of fixed nitrogen to the atmosphere as N_2 gas, either through canonical denitrification or anaerobic ammonium oxidation (anammox). However, inefficiencies in the microbially driven processes of nitrification and denitrification, are known to produce the greenhouse gas N_2O. Also, since nitrification produces the highly mobile anion nitrate, in terrestrial and aquatic compartments, this process may be a significant contributor of Nr delivery via rivers to the coastal ocean (Gruber and Galloway, 2008), where it can contribute to well-documented instances of coastal eutrophication (Rabalais, 2002), significant coastal denitrification (Seitzinger *et al.*, 2006), or even particulate organic carbon export to the deep ocean (Hales *et al.*, 2006; Wetz *et al.*, 2006).

Until recently, ammonia oxidation – the first and rate-limiting step in nitrification – was widely believed to be carried out by a few groups of chemolithotrophic ammonia-

oxidizing bacteria (AOB) in the *β* and γ subdivisions of the *Proteobacteria*. With the discovery of ammonia oxidation in the domain *Archaea*, ammonia monooxygenase (*amo*)-containing *Crenarchaeota* have been found to be widespread and abundant in a variety of aquatic and terrestrial environments (Francis *et al.*, 2005), including soils (Leininger *et al.*, 2006; He *et al.*, 2007; Shen *et al.*, 2008; Nicol *et al.*, 2008), estuaries (Francis *et al.*, 2005; Caffrey *et al.*, 2007; Mosier and Francis, 2008), and open ocean water columns (Wuchter *et al.*, 2006; Mincer *et al.*, 2007; Beman *et al.*, 2008), suggesting a significant relative contribution by the ammonia-oxidizing archaea (AOA) to nitrification in those systems.

Many of these studies examining the relative abundance of AOA and AOB have used quantitative PCR (qPCR) to assay the proteobacterial genes encoding the alpha subunit of ammonia monooxygenase (*amoA*) alongside their putative archaeal homolog. In marine pelagic environments, AOA are found to be consistently more abundant than AOB (Mincer *et al.*, 2007; Coolen *et al.*, 2007; Lam *et al.*, 2007) with some studies showing additional biogeochemical evidence for significant archaeal nitrification (Wuchter *et al.*, 2007; Beman *et al.*, 2008; Santoro *et al.*, 2010). In estuarine (Caffrey *et al.*, 2007; Mosier and Francis, 2008; Moin *et al.*, 2009; Santoro *et al.*, 2008), soil (Shen *et al.*, 2008; Jia and Conrad, 2009), and wastewater systems (Wells *et al.*, 2009), AOA do not consistently outnumber AOB, with some studies demonstrating AOB numerical dominance. In the few studies that included biogeochemical measurements, the evidence for a significant contribution of AOA is unclear and suggests a complex set of relationships determining niche partitioning, with differential ammonia oxidation kinetics being a probable main contributor (Martens-Habbena *et al.*, 2009).

Studies examining the relative abundances of ammonia-oxidizers in estuaries have primarily focused on sediment populations (Caffrey *et al.*, 2007; Mosier and Francis, 2008; Moin *et al.*, 2009). However in large rivers and estuaries, due to their smaller surface to volume ratio, water column nitrification is likely to be more important than benthic nitrification (Brion *et al.*, 2000; Billen, 1975; Berounsky and Nixon, 1993). In this study we examined the distribution and abundance of AOA and ammonia-oxidizing betaproteobacteria (β-AOB) via qPCR analyses of *amoA* genes along physicochemical and temporal gradients in the water columns of the lower Columbia River Estuary ecosystem. The Columbia River is the second largest river in the United States with a drainage basin of 658,726 km^2 and is the largest source of freshwater to the northeastern Pacific Ocean. Spatial variability was examined, along with environmental parameters, from samples collected during a ~160 km transect encompassing 9 stations. Temporal variability was examined monthly over a year-long period at a site where autonomous biogeochemical measurements were collected at an hourly timescale (SATURN-05). During the time series study, water quality indicators and natural abundance stable isotope ratios ($\delta^{15}N$) of nitrate were determined to better understand seasonal inorganic N cycling in the Columbia River watershed. Finally, nitrification activity was measured at this station using ^{15}N-labelled tracer and nitrification inhibitor additions during an instance of observed *in situ* nitrate increase.

3.3 Results

3.3.1 *Spatial survey - hydrographic and biogeochemical setting*

Physical, chemical, and biological spatial variability were examined during a research

cruise in July 2008 that included nine stations between the Columbia River estuary and

the urbanized reaches of the Willamette River (referred to as the Columbia River System

(CRS)). Sampling spanned the range of salinities reflective of an estuary-to-river

sampling gradient (Figure 3.1, Table 3.1). Four stations (A-D) were located at various

points within the ocean influenced reaches of the estuary, and thus received differing

amounts of salt water influence, due to physical locations relative to the estuary mouth, as

well as sampling times (flood/ebb tide conditions). Three stations (E-G) were located

along the tidally influenced regions of the Columbia River and two stations (H, I) were

located along the tidally influenced reaches of the Willamette River. Since summers

along the Oregon continental shelf are typified by upwelling and low river discharge,

pulses of nutrient-rich seawater are tidally entrained into coastal bays and estuaries

during these periods (Sigleo and Frick, 2007; Bruland *et al.*, 2008). During the survey

period, bottom waters in the estuary were similar to upwelled coastal waters (cold,

nutrient rich, and oxygen poor) while surface waters in the estuary and river exhibited

high chlorophyll *a* values and more nutrient poor conditions (Table 3.2). Silicate was

higher in fresh waters in comparison to ocean-influenced waters. The Willamette River

exhibited the highest nutrient concentrations and yet the lowest chlorophyll *a* values of

all the riverine sampling sites.

3.3.2 *Temporal survey: hydrographic and biogeochemical setting*

Temporal variability between July 2009 and August 2010 was examined at a site on the Columbia River, near the Beaver Army Terminal (river mile 53; Figure 3.1, Table 3.1). This location is where an *in situ* biogeochemical station (SATURN-05) is located at 2.5m depth and collects hourly measurements (Figure 3.1). To complement the relevant measurements made by the instrument package (temperature, dissolved oxygen, chlorophyll, CDOM, turbidity, and nitrate), samples were collected and analyzed for chlorophyll, phosphate, silicic acid, ammonium, nitrite, and nitrate.

Hydrography and biogeochemistry in Northeastern Pacific rivers are strongly influenced on a seasonal basis by precipitation (Peterson *et al.*, 1984; Colbert and McManus, 2003; Sigleo *et al.*, 2005). Peak rainfall, occurring in the winter months, and snowmelt in the spring, combine to create high discharge periods that transport dissolved nutrients and terrestrial sediments down rivers and into estuaries. During winter months, Columbia River discharge is significantly influenced by the large excess of precipitation provided by the mild, wet winters in the coastal sub-basin which is divided from the eastern sub-basin by the Cascade Range. However, Columbia River discharge is highest during April to July, when most of the runoff occurs as snowmelt derived from the eastern sub-basin. Summer months are characterized by low river discharge and the concomitant drawdown of nutrients by primary producers. Indeed, these trends were observed in the year-long study (Figure 3.4), with increasing river discharge as winter progressed, resulting in higher nutrient concentrations, along with turbidity and CDOM measured *in situ*. These periods of increased river discharge from November to April were greatly influenced by the Willamette River, the largest tributary in the coastal sub-

basin, with contributions between 28 – 37% to the total Columbia River flow at peak

discharge events. Notably, agricultural and urban land-use comprises 22% and 6%,

respectively, of the Willamette River basin, where nearly 70% of Oregon's population

resides (Carpenter and Waite, 2000). Chlorophyll started to increase gradually in late

February, and was followed by two large blooms from late March to early May (Figure

3.4e). These increases in chlorophyll resulted in the continuous overall drawdown of all

nutrients, except for nitrite, which reached its highest levels in April, during the middle of

the second and largest bloom (Figure 3.4b). Maximum Columbia River discharge

occurred from April to July 2010, with the percent contribution of the Willamette River

progressively decreasing along with the delivery of nutrients (Figure 3.4d). Even though

nutrients were decreasing based on discrete measurements, continuous nitrate

measurements reflected this decrease but also exhibited pulses of nitrate that were not

captured by sampling and which were inversely correlated to chlorophyll values (Figure

3.4e).

3.3.3 *Spatial variability of AOA and β-AOB abundance*

Abundance of archaeal and betaproteobacterial *amoA* genes was determined at the 9

aforementioned sites in the CRS from water samples obtained from surface (1m depth)

and bottom (1m above bottom) waters (Figure 3.2a). The AOA *amoA* gene copy numbers

ranged from 7 to 4.37 x 10^3 copies ml^{-1}, and 1.46 x 10^3 to 9.76 x 10^5 copies per

microgram DNA. β-AOB *amoA* ranged from 3 copies ml^{-1} to 23 copies ml^{-1}, and 450 to

4.94 x 10^3 copies per microgram DNA. β-AOB *amoA* was not detectable at one site in the

Columbia River at surface depth. AOA *amoA* gene abundance was greater in bottom

water column samples than in surface waters in all but three riverine sites (t-test, p <

0.05). This difference in bottom and surface waters was magnified in instances where the bottom water column experienced salinity intrusions (Tukey test, $p < 0.001$), with bottom waters averaging 1.14×10^3 copies ml^{-1} and surface waters averaging 81 copies ml^{-1}. AOA *amoA* gene abundances were thus greatest in the bottom water samples in the estuary experiencing salinity intrusions. Due to estuarine circulation influences, surface waters during bottom water salinity intrusions remained fresh, and these samples exhibited AOA *amoA* gene abundances that were significantly higher than abundances in estuarine surface waters during freshwater dominated periods, and in surface waters of the Willamette River (Tukey test, $p < 0.05$), but not higher than abundances in surface waters of the Columbia River. Combining surface and bottom water samples, AOA *amoA* gene abundances were lowest in the Columbia River estuary during freshwater dominated periods and in the Willamette River (average abundance of 37 copies ml^{-1}).

β-AOB *amoA* gene abundance did not exhibit a wide range of values and did not differ as much as AOA *amoA* gene abundance, with respect to depth or hydrodynamic setting (Table 3.2). β-AOB *amoA* gene abundance was greater in bottom water column samples at four sites (t-test, $p < 0.05$), two of which were instances where salinity was relatively high. When combining β-AOB *amoA* gene abundances, however, bottom water samples were significantly different from surface waters (Tukey test, $p < 0.05$) but not as significant as AOA *amoA* gene abundances (Tukey test, $p < 0.001$). When pooling β-AOB *amoA* gene abundances into samples from different hydrodynamic settings, only differences in depth were observed within the Columbia River samples (Tukey test, $p < 0.05$) and no differences were observed between hydrodynamic settings.

AmoA gene abundance was significantly greater for AOA than for β-AOB in all examined samples (paired t-test, p < 0.05), except for four, two of which were at a site in the Willamette River (Figure 3.2b). AOA *amoA* genes were on average 144 times more abundant than β-AOB *amoA* genes in salinity influenced bottom waters in the estuary. In the Columbia River, including surface and bottom water depths, AOA *amoA* gene copies were on average 21 times more abundant than β-AOB *amoA*. Bottom and surface waters during intermediate bottom water salinities of 9-26 psu exhibited an average AOA:β-AOB *amoA* gene copy ratio of 233 and 36, respectively. In all other samples, excluding the cases in which the abundance of β-AOB *amoA* and AOA *amoA* was not significantly different, the AOA: β-AOB *amoA* gene copy ratio averaged about 4.

Canonical correspondence analysis (CCA) showed that Axes 1, 2, and 3 explained about 26%, 8%, and 4%, respectively, of the variability in the data set (Figure 3.3). Axis 1 explained most of the variability associated with the AOA:β-AOB *amoA* gene copy ratio, indicating that ammonium, oxygen, and light transmissivity were the dominant factors, in decreasing order. Axis 2 explained most of the variability associated with AOA *amoA* gene copy numbers, with salinity, oxygen, and temperature being the dominant factors. Axis 3 (not shown) explained most of the variability associated with β-AOB *amoA* gene copy numbers with chlorophyll and nitrite being the dominant factors. Without the outlier influences of the Willamette River, Pearson correlation coefficients (Table A.1) displayed significant positive correlations between AOA *amoA* gene abundance and the AOA:β-AOB *amoA* gene copy ratio (r = 0.908, p < 0.001), which were both significantly and positively correlated to salinity (p < 0.05) and nitrate (p < 0.005); on the other hand they were significantly and negatively correlated to temperature

($p < 0.05$), oxygen ($p < 0.01$) and chlorophyll ($p = 0.002$). When analyzed individually and by removing the outlier influences of the Willamette River samples, AOA *amoA* gene copies and the AOA:β-AOB *amoA* gene copy ratio were both found to be significantly and positively correlated with ammonium, nitrite, and nitrate (all: $p < 0.05$) with AOA *amoA* gene abundance exhibiting stronger correlations (Figure A.1; all: $p < 0.005$). Also, significantly negative correlations were found between AOA *amoA* gene abundance and the AOA:β-AOB *amoA* gene copy ratio with light transmissivity when analyzed individually and in separate hydrodynamic compartments. AOA *amoA* gene abundance was significantly correlated to light transmissivity (Figure A.1d) in ocean-influenced bottom waters ($r = -0.849$, $p = 0.016$) and in freshwater samples excluding those from the Willamette River ($r = -0.465$, $p = 0.045$). The AOA:β-AOB *amoA* gene copy ratio was only significantly correlated to light transmissivity in freshwater samples excluding the Willamette River ($r = -0.694$, $p = 0.001$). No significant correlations were found with β-AOB *amoA* gene abundances.

3.3.4 *Temporal variability of AOA and β-AOB abundance*

AOA and β-AOB *amoA* gene abundance was quantified at the SATURN-05 station for the monthly samples collected between July 2009 and August 2010, for a total of 14 time points (Figure 3.4a). AOA *amoA* gene abundance values, for the time period studied, were comparable to the Columbia River samples taken during the spatial survey in July 2008, and ranged from 51 to 337 copies ml^{-1}. β-AOB *amoA* gene abundance values in this set of samples exhibited a wider range than those from the samples taken from the Columbia River in July 2008 (10^{0}-10^{1}) and ranged from 7 to 204 copies ml^{-1}. AOA *amoA*

abundance in samples taken in July and August 2009 were not significantly different than abundance values collected from the three sites in the Columbia River in July 2008 (t-test, $p < 0.05$). This similarity was not observed for β-AOB *amoA* copy numbers, with about 3-fold higher values found in Summer 2009 samples, but was observed between samples taken in the Summer of 2010 (June and August) and July 2008 (t-test, $p < 0.05$).

AOA *amoA* gene copy numbers were greater than β-AOB *amoA* gene copy numbers in most samples examined, with the exception of 4 samples, only one of which was higher for β-AOB (paired t-test, $p < 0.05$). The AOA:β-AOB *amoA* gene copy ratio ranged from 0.39 to 34, with the lowest ratio occurring in January 2010, during the period of highest discharge and concentrations of dissolved nutrients, when β-AOB *amoA* gene copy numbers outnumbered AOA *amoA* by about 2.5-fold. This was also a period when Willamette River discharge had its highest influence in terms of percent contribution to Columbia River discharge (maximum of 37%). Highest ratios of AOA:β-AOB *amoA* were consistently observed in the late spring and summer months when nutrients and Willamette River contribution to total discharge were at their lowest levels.

Principal components analysis of 11 physical and biogeochemical properties effectively grouped the time points into three general categories: 1) high nutrients and high discharge associated with winter precipitation, 2) spring months characterized by high chlorophyll, N:P ratios, and nitrite, and 3) summer months with high temperatures and low nutrients (Figure 3.5). Forty-eight percent of the variation was described by principal component one with nitrate, phosphate and ammonium being the main causes of variability and which effectively grouped the high nutrients and discharge sampling points. Directly anti-correlated to these points on axis 1 were the summer and early fall

sampling points. Approximately 20% of the variation was described by axis 2 with the

N:P ratio and chlorophyll being the dominant eigenvectors and thus, grouping the early

spring time points. A Pearson correlation matrix with AOA *amoA* gene copies, β-AOB

amoA gene copies, AOA:β-AOB *amoA* ratios, and nutrients, revealed significant co-

correlation between ammonium and nitrate (r = 0.802, p = 0.016) as well as phosphate (r

= 0.792 , p = 0.021). In addition, it showed that the AOA:β-AOB *amoA* ratio was

significantly and positively correlated to AOA *amoA* gene abundance (r = 0.822, p =

0.009) but not to β-AOB *amoA* gene abundance. When the AOA:β-AOB *amoA* ratio was

analyzed individually with each environmental variable, ammonium (r = -0.732, p =

0.003), phosphate (r = -0.577, p = 0.031), and discharge (r = 0.540, p < 0.05) were found

to be significant. AOA *amoA* gene abundance was also found to be significantly and

positively correlated to discharge (r = 0.757, p = 0.002). On the other hand, when β-AOB

amoA gene abundance was analyzed individually with each environmental variable,

nitrate, ammonium, phosphate, silicic acid, turbidity, as well as the percent contribution

of Willamette River discharge to Columbia River discharge, were all found to be

significantly and positively correlated (Pearson, p < 0.05).

3.3.5 *Natural abundance of $\delta^{15}N$ in NO_3^- and temporal variability*

Natural abundance values of ^{15}N in nitrate are reported using delta (δ) notation in units of

per mil (‰):

$$\delta^{15}N_{sample} = ((^{15}N/^{14}N)_{sample}/(^{15}N/^{14}N)_{reference} - 1) \times 1000‰$$

where the reference is N_2 in air. The $\delta^{15}N$ values of nitrate collected monthly from the

time series site thus ranged from 2.2 to 7.8 ‰, with the highest values occurring in

Summer and Fall 2009 (Figure 3.4c). From then on, $\delta^{15}N$ values in nitrate decreased with the large pulses of nitrate, and continued to decrease, as nitrate decreased with the onset of the spring phytoplankton blooms. When analyzed individually, nitrate and the $\delta^{15}N$ of nitrate were, in fact, significantly and negatively correlated (Figure 3.6) (r = -0.663, p = 0.014). In 4 out of 13 examined time points, the $\delta^{15}N$ value decreased while nitrate increased, when compared to the previous time points (Figure 3.4c, gray boxes). Also, in 3 other time points, the $\delta^{15}N$ value decreased while nitrate decreased, when compared to the previous time point (Figure 3.4c: October, late February, April). These points were coincident with high chlorophyll a concentrations indicative of phytoplankton blooms, but in general, chlorophyll a values were negatively correlated with nitrate concentrations (r = -0.671, p = 0.012) and phaeophytin concentrations (r = -0.732, p = 0.004) while being positively correlated with $\delta^{15}N$ values in nitrate (r = 0.507, p = 0.093). To punctuate the importance of the $\delta^{15}N$ values to the temporal data set, the PCA analyses mentioned above, indicate that the natural abundance of $\delta^{15}N$ explained approximately 10% of the variability in the data set in Axes 3 and 4 combined, which in total combined to explain roughly 23% of the total variability observed in the data set.

3.3.6 *Nitrification rate experiments*

Nitrification rate measurements were made from surface water collected at the time series site in August 2010, during a period of observed *in situ* nitrate increase (Figure 3.7) coincident with increased sky cover and precipitation. $^{15}NH_4^+$ was added to four incubation bottles: two with whole river water and two with whole river water and the nitrification inhibitor allylthiourea (ATU). This experimental setup was replicated with

$^{15}NO_3^-$ and nitrification rates calculated using the Blackburn-Caperon isotope-dilution model (Clark *et al.*, 2007). Averages and standard deviations were derived from rates calculated for each time point and bottle, with outlier results not included in the analysis. Nitrification was detected and measured as ^{15}N-$(NO_2^- + NO_3^-)$ production in the $^{15}NH_4^+$ labelled incubation bottles and ^{15}N-$(NO_2^- + NO_3^-)$ dilution in the $^{15}NO_3^-$ labelled incubation bottles; nitrification rates derived from each method were 246 ± 105 (n = 3) and 229 ± 115 (n = 5) nM day^{-1}, respectively. Production of $^{15}NO_3^-$ in $^{15}NH_4^+$-labelled and ATU-treated bottles was not significantly different from zero, with one bottle yielding a rate of 30 nM day^{-1} and the second bottle completely inhibited. However, dilution of $^{15}NO_3^-$ in $^{15}NO_3^-$-labelled and ATU-treated bottles was observed, yielding a wide range of nitrification rates. Bottle 1 yielded rates of 797 nM day^{-1} while bottle 2 yield rates of 190 nM day^{-1}, and both combined to create an average and standard deviation of 493 ± 430 nM day^{-1}. *In situ* nitrate increases during this period was roughly 800 nM day^{-1} - about 3-fold greater but on the same order as the chemolithoautotrophic nitrification rate measurements as measured by $^{15}NH_4^+$ tracer additions.

3.4 Discussion

3.4.1 *Longitudinal and depth distributions of AOA and β-AOB and relationship to environmental variables*

Since previous studies on AOA *amoA* gene abundances in estuaries have focused on sediment populations, it is hard to compare the copy numbers derived here to other studies. Estuaries are essentially defined by the confluence and mixing of freshwater and

saltwater end members, and therefore previous studies from those source environments can be used as potential markers. Indeed, Crump and Baross (2000) concluded from archaeal 16S ribosomal RNA (rRNA) clone libraries, that archaea in the Columbia River estuary were primarily allochthonous in origin. Assuming salinity influenced bottom water samples in this study came from a mixture of oligotrophic surface ocean waters and upwelled nitrate rich deep waters, with AOA *amoA* copy numbers of 10^{-1}-10^{0} copies ml^{-1} (Mincer *et al.*, 2007; Church *et al.*, 2010; Santoro *et al.*, 2010) and 10^{4}-10^{5} copies ml^{-1} (Mincer *et al.*, 2007; Beman *et al.*, 2008; Santoro *et al.*, 2010) respectively, the range of values we found in these samples (10^{2}-10^{3} copies ml^{-1}) is not altogether unexpected. The range of values that were observed in the Willamette River, the Columbia River and freshwater dominated instances in the estuary (10^{0}-10^{2} copies ml^{-1}) were on the low end of values found for recent studies quantifying AOA *amoA* in rivers (10^{0}-10^{4} copies ml^{-1}) (Herfort *et al.*, 2009; Liu *et al.*, 2010), although the rivers examined in those studies exhibited in general much higher nutrient concentrations than the river systems studied here. When considering the range of values of AOA *amoA* abundance as gene copies per microgram DNA, the values found in this study fall in the middle range of AOA *amoA* gene abundance measurements from the San Francisco Bay (10^{2}-10^{6} copies per microgram DNA; Mosier *et al.*, 2008). The β-AOB *amoA* gene abundance values found in the spatial survey are very similar to those recently found in the Dongjiang River, China (10^{0}-10^{1} copies ml^{-1}; Liu *et al.*, 2010).

Depth profiles of archaeal *amoA* genes demonstrate a consistent and marked difference between samples taken from bottom and surface water samples throughout the CRS. β-AOB *amoA* genes also demonstrated this pattern, although much more weakly

and less consistently. There are a couple of possible explanations for the higher observed *amoA* gene abundances at near-bottom depths. One possibility is an effect of photoinhibition on ammonia oxidation and growth of ammonia-oxidizing bacteria, which has been observed in marine, estuarine and freshwater environments (Olson, 1981; Lipschultz *et al.*, 1985; Ward, 1987; Horrigan and Springer, 1990) and may also occur in the Columbia River. It is, as of yet, unclear whether AOA are inhibited by light, although a recent study in the central Pacific Ocean (Church *et al.*, 2010) demonstrated elevated AOA *amoA* gene expression in the euphotic zone relative to the mesopelagic zone, suggesting that marine AOA may be less sensitive to light than AOB. However, this depth-related increase in gene expression may not have reflected an increase in per cell ammonia oxidation activity.

A second possible explanation for higher AOA *amoA* gene copies in bottom water samples is the persistence of 'permanently suspended particles' (Plummer *et al.*, 1987; Crump and Baross, 1996) at bottom depths that are a consequence of estuarine turbidity maxima (ETM) or from the strong tidal influence throughout the system, including the Willamette River. Suspended particles can be organic-matter rich, allow for NH_4^+ adsorption (Boatman and Murray, 1982), decrease light penetration and have increased residence times in estuaries due to ETM (Jay *et al.*, 1990; Reed and Donovan, 1994). They have been shown to be positively correlated to potential nitrification rates in estuaries (Brion *et al.*, 2000), and rivers (Xia *et al.*, 2009), and are one of the main factors postulated to explain greater nitrification rates in estuaries and rivers relative to coastal seas and the open ocean (Kaplan, 1983; Horrigan and Springer, 1990 and references therein). Crenarchaeota, detected by CARD-FISH and highly correlated to AOA *amoA*

gene abundance, have been observed to be associated with particles in the North Sea (Wuchter *et al.*, 2006). Indeed, we found light transmissivity, another measure of turbidity, to be significantly and negatively correlated to AOA *amoA* gene abundance in salinity-influenced and freshwater samples, excluding the Willamette River, but not to β-AOB *amoA* abundance. Nevertheless, this significant depth-related difference in *amoA* gene copy numbers is not predictive of higher ammonia-oxidation rates at lower depths, since a measure of gene abundance only reflects genetic potential or past activity and not *in situ* activity.

In general, during the spatial survey, the AOA:β-AOB *amoA* ratio increased with increasing salinity, with the highest ratios (average = 233, n = 3) observed at intermediate salinities between 9-26 psu and the lowest ratios (average = 4.1, n = 10) observed during the freshwater dominated instances in the estuary and in the Willamette River. Only in four freshwater samples were AOA *amoA* gene copy numbers not greater than β-AOB *amoA* copy numbers, and none of the samples had greater β-AOB *amoA* gene abundance. This is in contrast to recent reports from estuarine environments, in which gene copy ratios decreased, and in some cases became negative (i.e. β-AOB outnumbered AOA), as salinity increased (Caffrey *et al.*, 2007; Mosier *et al.*, 2008; Bernhard *et al.*, 2010; Santoro *et al.*, 2010). Ratios in those studies ranged from less than 1 to over 100, compared to a similar minimum ratio of less than 1 and a maximum ratio of approximately 339 found here. Moin *et al.* (2009) found a maximum ratio of approximately 215 in sediments of the least salt tolerant salt marsh studied. Similar to Caffrey *et al.* (2007), who found a positive correlation between AOA *amoA* gene abundance and salinity and not between β-AOB *amoA* gene abundance and salinity, we

found a positive correlation between the AOA:β-AOB *amoA* ratio and salinity (Pearson, $p < 0.001$).

Since AOA *amoA* gene abundances are often 2 to 3 orders of magnitude greater than β-AOB *amoA* abundances in most studies in the open ocean (Wuchter *et al.*, 2006; Mincer *et al.*, 2007; Beman *et al.*, 2008; Beman *et al.*, 2010; Santoro *et al.*, 2010), one might expect to see increasing AOA:β-AOB *amoA* ratios with increasing salinity, as we found in this study and as Caffrey *et al.* (2007) found in 5 of the 6 estuaries they examined. The discrepancy between the results reported here and in other recent estuarine studies (Santoro *et al.*, 2008; Mosier *et al.*, 2008; Bernhard *et al.*, 2010), therefore imply that a more complex set of variables may influence the relative abundance of AOA and β-AOB, and hence, their contributions to ammonia-oxidation, in estuarine settings. It is possible, in light of the recent report that the AOA *N. maritimus* has an ammonia affinity of up to 2 orders of magnitude greater than that of cultivated AOB (Martens-Habbena *et al.*, 2009), that ammonia concentrations may play a large role in determining the relative distributions of different ammonia-oxidizing organisms. For example, although no correlations were found between ammonia concentrations and the AOA:β-AOB *amoA* gene copy ratio, in the San Francisco Bay study by Mosier *et al.* (2008), the highest nitrate, nitrite and ammonia concentrations were found in the low flushing and WWTP-effluent receiving South Bay, and coincided with the lowest AOA:β-AOB *amoA* ratios. In fact, the strong correlations found for AOA *amoA*, β-AOB *amoA*, and the AOA:β-AOB *amoA* ratio with C:N ratios may have been driven by these differences in nitrogen loading between the North and South Bay. Similarly, in the study of six estuaries by Caffrey *et al.* (2007), the β-AOB *amoA* gene copies were greater than

those of AOA only at one estuary, Weeks Bay, which had the highest ammonium concentrations as well as being highly sulfidic.

In the spatial portion of this study, the AOA:β-AOB *amoA* ratio was found to be significantly correlated to nitrate which was co-correlated with salinity ($r = 0.877$, $p < 0.001$). Salinity was also found to be significantly and negatively co-correlated with oxygen ($r = -0.987$ $p < 0.001$) and temperature ($r = -0.991$, $p < 0.001$). However, nitrate concentrations continued to fluctuate, along with the AOA *amoA* gene copies and the AOA:β-AOB *amoA* gene copy ratio all the way up to the Willamette River. Ammonium and nitrite, when analyzed individually and without the outlier influences of the Willamette River, were found to be significantly correlated to AOA *amoA* gene copies (Figures A.1a – c) and the AOA:β-AOB *amoA* gene copy ratio, and yet were not significantly co-correlated with salinity. Indeed, the CCA analyses, which included all samples, show that ammonium was the most dominant factor explaining the variability in the AOA:β-AOB *amoA* ratio throughout the CRS in July 2008.

Ammonium concentrations, as measured by the indophenol-blue method, ranged from 0.4 to 5.9 μM [NH_4^+], with the highest concentrations consistently occurring in the Willamette River (where the AOA:β-AOB *amoA* gene copy ratios were some of the lowest). Some high NH_4^+ concentrations did occur in the estuary that were associated with the confounding effects of upwelled and nutrient rich deep ocean waters. A subset of the samples was measured using the fluorometric ammonium assay (Holmes *et al.*, 1999), which indicated that results were overestimated at the lower end of the ammonium range (Figure A.1a – b). Nevertheless, the ammonium concentrations found in this portion of the study are for the most part in the range of the maximum specific growth

rate (V_m) of *N. maritimus* (~1 μM [NH_4^+]) and consistently below the half-saturation

constant (K_m) of characterized AOB (> 10 μM [NH_4^+]) (Martens-Habbena *et al.*, 2009).

The discrepancy reported here concerning the relationship between the AOA:β-AOB

amoA gene copy ratio and salinity, compared to other recent studies examining the

relative abundances of ammonia-oxidizers in estuaries, may derive from the fact that this

study is the first conducted in an estuarine water column, where dissolved and particulate

substrates may be more diffuse and transient. On the other hand, previous studies have

focused on ammonia-oxidizer populations in estuarine sediments, which are typically

organic matter and particle rich, providing ample substrate for ammonium

remineralization and adsorption.

Additionally, it is possible that the low AOA:β-AOB *amoA* ratios observed in the

CRS were a result of ammonium competition between AOA with phytoplankton and

heterotrophic bacteria, cultured representatives of which have K_m below 1 and 10 μM

[NH_4^+], respectively. Including Willamette River samples, the AOA:β-AOB *amoA* gene

copy ratio was found to be negatively correlated to chlorophyll (r = -0.531), and when

analyzed individually, was found to be significant (r^2 = 0.398, p = 0.029). Although the

eutrophic Willamette River exhibited the highest nutrient concentrations of all examined

sites, it also exhibited relatively low chlorophyll values. Total bacterial counts, as

opposed to chlorophyll, have been shown to be at times more indicative of eutrophic

conditions (Wang *et al.*, 2010), and although total bacterial counts were not available for

this study, the possibility of high nutrients being the explanation for the lower AOA:β-

AOB *amoA* gene copy ratios observed in the Willamette River is intriguing.

3.4.2 *Temporal distribution of AOA and β-AOB abundances and relationship to environmental variables*

During the year-long time series, a significant negative correlation between AOA:β-AOB *amoA* ratios and ammonium stands in stark contrast to the significantly positive correlations between β-AOB *amoA* gene abundance, ammonium and other nutrients. As ammonium and other nutrients progressively increased and fluctuated from summer 2009 to January 2010, β-AOB *amoA* gene copies fluctuated in near-perfect tandem, while AOA *amoA* gene abundance barely fluctuated and only increased once from the previous sampling point – during the first high discharge event between the October and early December 2009 time points. From early February 2010 on, however, as ammonium, other nutrients, and the percent contribution of Willamette River discharge gradually decreased, AOA *amoA* gene abundance gradually increased while β-AOB *amoA* gradually decreased.

This set of correlations may reflect niche partitioning of archaeal and bacterial ammonia-oxidizers based on ammonia oxidation kinetics and ammonium availability (Martens-Habbena *et al.*, 2009), whereby low ammonium concentrations lead to AOA dominance and high ammonium concentrations lead to β-AOB favorable conditions. From April to August 2010, when ammonium concentrations fell consistently below 1 μM [NH_4^+], AOA:β-AOB *amoA* gene copy ratios were at their highest during the time period studied and averaged around 20. This contrasts to AOA:β-AOB *amoA* gene copy ratios that averaged ~1.5 between September 2009 and March 2010, when ammonium concentrations were always above 1 μM [NH_4^+], except for the October 2009 time point, which coincidentally resulted in a β-AOB *amoA* gene copy decrease, but no change in

AOA *amoA* gene copies. Although the AOA:β-AOB *amoA* gene copy ratio was lower during the high nutrient and discharge time points, AOA *amoA* gene copies were greater than β-AOB *amoA* gene copies in all but five sampling points, only one of which exhibited higher β-AOB *amoA* gene abundance.

These points of β-AOB *amoA* numerical parity and dominance were almost always associated with a high turbidity event prior to the sampling point and would decrease always immediately during the following sampling point. Since β-AOB *amoA* gene abundance was also highly correlated to the percent contribution of the Willamette River to the Columbia River discharge, it is possible that these instances of β-AOB *amoA* numerical parity and dominance were short-lived episodic events that were a byproduct of terrestrial runoff or WWTP effluent from the eutrophic Willamette River watershed. AOA *amoA* gene abundance on the other hand, rarely fluctuated during this time period, but started to increase as ammonium concentrations decreased. AOA *amoA* gene abundance was, however, found to be significantly correlated to gross Columbia River discharge, which reached its highest levels from April to June 2010 as a result of snowmelt from the Cascade Range and other highlands eastward. A difference in the hydrological and biogeochemical characteristics of each water body as well as the land-use characteristics of its watershed may therefore be predictive of the relative abundances of ammonia oxidizers in this and other similar systems. Since only *amoA* gene abundance data was gathered, information that may be derived about the source of these organisms (allochthonous vs. autochthonous) from sequence derived phylogenies, or relative activity from gene transcript abundances was not available.

Unlike the other dissolved nutrients measured, nitrite concentrations did not decrease immediately after the highs of January and early February 2010 but instead continued to increase and fluctuate until April 2010 in tandem with AOA *amoA* gene copies. The highest nitrite concentrations were also coincident with phytoplankton blooms. Nitrite maxima have been found to be coincident with phytoplankton biomass in river systems (Lipschultz *et al.*, 1985, 1986) and right below the chlorophyll maxima, at the base of the euphotic zone, in the open ocean. In fact, the primary nitrite maximum (PNM) in open ocean systems has been the subject of considerable research (reviewed by Lomas and Lipschultz, 2006) and its formation and maintenance is thought to be dominated by either differential light inhibition of ammonia- and nitrite-oxidizers (Olson, 1981) or the reduction of NO_3^- to NO_2^- by phytoplankton under light limitation (Vaccaro and Ryther, 1960; Kiefer *et al.*, 1976) or increased irradiance (Olson *et al.*, 1980; Lomas and Glibert, 1999, 2000) Since the samples examined here were taken at surface depths and at 3m below the surface, the reduction of NO_3^- to NO_2^- by phytoplankton under light limitation can be ruled out. It is therefore unclear whether these tandem fluctuations between NO_2^- concentrations and AOA *amoA* gene abundance was reflective of ammonia oxidation activity at surface depths and differential light inhibition of nitrite-oxidizing bacteria (NOB), since light inhibition of AOA has not been conclusively demonstrated, NOB were not quantified, and neither transcript and nitrification rate measurements were conducted for these samples.

3.4.3 *Temporal variability of $\delta^{15}N$ in nitrate in the Columbia River*

Although N isotopic compositions of N-containing compounds in terrestrial runoff and atmospheric precipitation are poorly constrained (Sigman *et al.*, 2009), the month-to-month fluctuations as well as the overall trend of the $\delta^{15}N$ of nitrate and NO_3^- relationships in the Columbia River time-series suggest that either (i) nitrification may be a dominant process *in situ* or (ii) the signal was due to terrestrial nitrification carried into the river by runoff. A significant and negative correlation between nitrate and the $\delta^{15}N$ of nitrate is consistent with nitrification since the process results in increased nitrate concentrations and low $\delta^{15}N$ values in nitrate due to the known isotopic fractionation factors involved in ammonia oxidation (12-38‰) (Casciotti *et al.*, 2002; Sigman *et al.*, 2009). Additionally, multiple linear regression analyses revealed that the AOA:β-AOB *amoA* ratio was significantly and negatively correlated to nitrate and to the $\delta^{15}N$ of nitrate (Figure A.2; $r^2 = 0.721$, $p < 0.001$), suggesting that AOA may be significant contributors to ammonia oxidation either *in situ* or as an integrative marker of runoff derived nitrification. Illustrating these relationships, are the 4 time points in which the $\delta^{15}N$ value decreased while nitrate increased (Figure 3.4, gray boxes), when compared to the previous time points. All 4 points, except for the point in August 2009, also saw a tandem increase either in AOA *amoA* copy numbers, β-AOB *amoA* copy numbers, or both. However, these 3 points were all associated with high turbidity and discharge events during or prior to sampling, thereby complicating efforts to decouple *in situ* and runoff-derived nitrification signatures. Nevertheless, the August 2009 time point was characterized by a decrease in the $\delta^{15}N$ value of nitrate and an increase in nitrate

concentration, while at the same time exhibiting low turbidity, low discharge, and a AOA:β-AOB *amoA* ratio of ~4.

Low concentrations of nitrate coupled with high δ^{15}N values in nitrate is also consistent with nitrate assimilation *in situ* as a result of phytoplankton nitrate uptake. Denitrification, either *in situ* or as a result of terrestrially derived signatures is another possibility. Since δ^{15}N values in nitrate were negatively correlated with gross Columbia River discharge (r = -0.554, p = 0.050) as well as the percent contribution of the Willamette River to the gross discharge (r = -0.635, p = 0.020), terrestrially derived signatures of denitrification activity are unlikely. On the other hand, chlorophyll *a* concentrations were positively correlated to δ^{15}N values in nitrate and significantly and negatively correlated to nitrate. Interestingly, there were 3 time points where nitrate concentrations and the δ^{15}N values in nitrate both decreased from the previous month's time point (Figure 3.4: October, late February, and April). Yet these points were also coincident with increased or high chlorophyll *a* and nitrite concentrations which suggest that despite nitrate uptake by phytoplankton, nitrification may have been the dominant process *in situ*. Another possibility is that the nitrate, if from land-derived sources, was so heavily nitrified terrestrially that it was not significantly impacted by nitrate assimilation upon delivery to the river. The N:P ratio during the entire study period never dropped below a Redfield ratio of 16:1 (Figure A.3), consistent with most studies in freshwater indicating that phytoplankton are typically phosphorous limited. Since phytoplankton derived primary production in the system was rarely nitrogen limited (i.e. nitrate was relatively abundant), a large isotope effect from nitrate assimilation would therefore have been likely (Sigman *et al.*, 2009). Furthermore, all 3 time points were characterized by a

decrease in β-AOB *amoA* copy numbers from the previous time point, while 2 time points exhibited increases in AOA *amoA* copy numbers when compared to the previous time point. Again, if nitrification was occurring *in situ*, this may imply that AOA were better able to compete for ammonium compared to the β-AOB, especially in the presence of phytoplankton (Martens-Habbena *et al.*, 2010). The fact that the N:P ratio never dropped below a Redfield ratio of 16:1 may suggest that planktonic N_2 fixers, such as cyanobacteria, are not particularly active in the Columbia River, and that most of the fixed reactive nitrogen fueling riverine phytoplankton blooms is supplied via terrestrial sources and nitrification.

3.4.4 *Nitrification in riverine surface waters*

The ^{15}N-based nitrification rates determined at the SATURN-05 site indicate that nitrification was occurring in riverine surface waters and most likely during day-time periods. A constant and linear *in situ* nitrate increase was observed to occur for roughly 6 days during a period of increased sky cover and precipitation, thereby theoretically allowing the phytoplankton to be at least partially inactivated and the nitrification signal to be detectable *in situ*. The rate of nitrate increase, for the time period simulated by the ^{15}N-tracer incubations, were on the same order of magnitude but were about 3 times greater *in situ*. There are several possible explanations for this perceived difference. One, is the fact that the ^{15}N tracer incubations were carried out in closed systems and in relatively small volumes (315 mL), such that the NH_4^+ pool provided by regeneration may have become limiting during the incubation period (Figure 3.8). On a related note, significant regeneration of NH_4^+ could have also lowered the atom percent ^{15}N of the

incubated NH_4^+ during the experiments, an effect that should have increased with incubation time (Vincent *et al.*, 1989; Clark *et al.*, 2008). Both of these factors would underestimate true nitrification rates, and indeed, we observed the highest nitrification rates as well as the highest NH_4^+ accumulation rates in the first time point (Figure 3.8) (t = 5.5 h). It is also possible that some of the nitrate increases could have been a result of advective transport from other potential sources upriver. However, this particular increase in nitrate was one of the few instances in the time-series that was not preceded by a large discharge or turbidity event. On the other hand, a large phytoplankton bloom was observed *in situ* from July to August 2010, after an influx of nitrate in June 2010 that was associated with Columbia River discharge and high turbidity. It is, therefore, quite likely that a large proportion of the observed *in situ* increase in nitrate was a product of *in situ* chemolithoautotrophic nitrification as a result of enhanced access to ammonia from decaying phytoplankton biomass.

The nitrification rates presented here are lower than those measured in other riverine systems (McCarthy *et al.*, 1984; Lipschultz *et al.*, 1986; Owens, 1986; Feliatra and Bianchi, 1993; Brion *et al.*, 2000; Cébron *et al.*, 2003). Those systems however, typically experience NH_4^+ loadings one to two orders of magnitude greater than the loadings found at SATURN-05. Also, many of the nitrification rates measured in those studies used, either in combination or independently, bulk changes in nutrient concentrations, non-limiting substrate conditions, or dark uptake of $H^{14}CO_3$, all of which have potential methodological constraints. The nitrification rate measurements obtained here, were conducted in the dark and used $^{15}NH_4^+$ and $^{15}NO_3^-$ tracer additions that were approximately 5.4% and 2.9% of ambient $[NH_4^+]$ and $[NO_3^-]$, respectively. The accurate

determination of starting *in situ* [NH_4^+] or $\delta^{15}NH_4^+$, which are difficult to make (Aminot *et al.*, 1997), is another essential element to obtaining accurate nitrification rate measurements. In this instance, [NH_4^+] was determined to be 0.35 μM immediately upon arrival in the lab using the fluorometric ammonium assay (Figure 3.8) (Holmes *et al.*, 1999). Yet, samples taken at the time of ^{15}N-tracer additions, about 2.5 h later, were measured using the classic indophenol-blue (IDB) method and yielded values of 1.6 μM NH_4^+. Significant NH_4^+ regeneration was clearly occurring but a possibility remained for the overestimation of [NH_4^+]. The two values were thus averaged to obtain a starting [NH_4^+]. Use of the [NH_4^+] values from the classic IDB method would have yielded higher nitrification rate estimates and vice versa for the fluorometric ammonium assay.

Initial AOA and β-AOB *amoA* gene copy numbers were quantified for this sample and exhibited abundance values of 233 ± 9 and 7 ± 3 copies ml^{-1} respectively. Assuming a maximum cell-specific ammonia-oxidation rate of 12 fmol $cell^{-1}$ d^{-1} for *Nitrosopumilus maritimus* (Martens-Habbena *et al.*, 2009), the only representative of the AOA in pure culture, the quantified AOA abundance values would yield an ammonia oxidation rate of 2.8 nM d^{-1}. After taking into account that β-AOB have on average 2.5 copies of *amoA* per cell (Norton *et al.*, 2002), and assuming a maximum cell specific ammonia-oxidation rate of 250 fmol $cell^{-1}$ d^{-1} for *Nitrosomonas europaea* (Martens-Habbena *et al.*, 2009), one of the best characterized and faster growing β-AOB, the quantified copies of β-AOB *amoA* would yield an ammonia-oxidation rate of 0.6 nM d^{-1}. These predicted ammonia-oxidation rates based on quantified *amoA* copy numbers are two orders of magnitude lower than those predicted using ^{15}N-tracer techniques and would require the same magnitude of difference in cell-specific ammonia-oxidation

activity for the AOA and β-AOB in the measured samples. A maximum cell specific ammonia oxidation rate of 1.2 pmol cell^{-1} d^{-1} as measured in a municipal wastewater treatment plant and presumably reflective of AOB (Limpiyakorn *et al.*, 2005) would still fall short by an order of magnitude. It is also possible that the primer sets used did not capture the entire population of AOA and β-AOB. The primer set used for the quantification of AOA *amoA* is very similar to the primer sets used in other recent quantitative studies of AOA (Wells *et al.*, 2009; Beman *et al*, 2010; Santoro *et al.*, 2010), but upon analysis, was found to have a single base-pair mismatch with the *amoA* gene sequence of *N. maritimus* in both forward and reverse primers. Furthermore, the single base pair mismatch in the reverse primer is near the 3′ end. It has been shown that a single base-pair mismatch near the 3′ end of a primer-target duplex can cause underestimations in gene copy numbers of up to 1000-fold (Bru *et al.*, 2008). Furthermore, β-AOB *amoA* has been well characterized phylogenetically (Rotthauwe *et al.*, 1997) and many strains exist in pure culture, but the possibility for undetected members of the group is still there. Also, AOB in the γ-proteobacterial sub-group were not quantified here, although they are generally in low abundance (Lam *et al.*, 2007), undetectable (Beman *et al.*, 2008), and more frequently found in marine environments (Ward and O'Mullan, 2002). Unfortunately, *amoA*-clone libraries were not obtained for this study.

Finally, ATU was found to completely inhibit nitrification as measured with the $^{15}NH_4^+$ tracer additions but not with the $^{15}NO_3^-$ tracer additions. ATU is a well known inhibitor of bacterial ammonia-oxidation and a previous study on an enriched thermophilic AOA did show some resistance to ammonia-oxidation inhibition in the

presence of 100 μM ATU (Hatzenpichler *et al.*, 2008). It is as of yet unclear how resistant the AOA present in the Columbia River are to ATU, and so, the scarcity of inhibitor data on cultured or enriched AOA makes extrapolation here about relative contributions of AOA and β-AOB to *in situ* ammonia-oxidation difficult. On the other hand, heterotrophic nitrifiers are considered to be generally insensitive to ATU (Wagner *et al.*, 1995) and several studies using $^{15}NH_4^+$ and $^{15}NO_3^-$ along with nitrification inhibitors, have used the differential accumulation of ^{15}N in the NO_3^- pool to infer the relative importance of heterotrophic nitrification (Schimel *et al.*, 1984; Pedersen *et al.*, 1999). That is, inhibition specific to chemolithoautotrophic nitrification would inhibit ^{15}N accumulation in the NO_3^- pool from $^{15}NH_4^+$ tracer additions whereas the use of organic carbon and nitrogen compounds by heterotrophic nitrifiers (Papen *et al.*, 1989; Daum *et al.*, 1998) would continue the dilution of the $^{15}NO_3^-$ pool even with inhibitors added. The nitrification rates derived from the $^{15}NH_4^+$ tracer additions were not statistically different from those derived from the $^{15}NO_3^-$ with ATU additions, indicating that both modes of nitrification are potentially of equal importance and when added together come quite close to the observed *in situ* nitrate increase. However, the nitrification rates derived from $^{15}NO_3^-$ tracer additions alone should reflect the addition of both of these modes of nitrification, and the fact that they don't may reflect the potential confounding effects of phytoplankton and bacterial nitrate assimilation which may cause an underestimation of nitrification rates by preferentially assimilating ^{14}N in nitrate (Sigman *et al.*, 2009).

3.5 Conclusions

To our knowledge, the year-long monthly time series described in this report is the most detailed record of AOA and β-AOB community dynamics in a large river to date. Correlations and tandem fluctuations of the AOA:β-AOB *amoA* ratio with ammonium, nitrite, δ^{15}N in nitrate, and discharge indicate a potentially large role of AOA in mesotrophic river nitrification, and a demonstrated niche partitioning of AOA and β-AOB associated directly with substrate availability as an indirect result of river discharge and watershed land-use factors. Conversely, since rivers integrate the landscape process in their watersheds, the tandem fluctuations of δ^{15}N in nitrate, AOA and β-AOB *amoA* gene copies may be indicators of previous nitrification activity associated with those landscape processes. Phylogenetic analysis along with transcript and nitrification activity measurements in a similar river time series would help elucidate the source of these inferred activities. Nevertheless, the AOA:β-AOB ratio may be used as another indicator of water quality, as β-AOB were found to be associated with discharge from the eutrophic Willamette River and AOA were found to be associated with low nutrient conditions. Nitrification was observed in samples collected from riverine surface waters where a concurrent *in situ* day-time nitrate increase was also determined, demonstrating measurable nitrification in euphotic surface waters most likely attributable to AOA and perhaps even heterotrophic nitrifiers. Temporal resolution of this process with respect to different periods and sources of discharge along with phytoplankton activity associated with seasonal fluctuations remains a promising area to further elucidate the interactions of AOA, other ammonia-oxidizers and their respective contributions to nitrification. Based on the nitrification rate experiment and tandem fluctuations between $\delta^{15}NO_3^-$, AOA, chlorophyll and the N:P ratio, it is quite possible, that the majority of

phytoplankton activity in the lower CR may be fueled by recycled nitrate, from nitrification, either *in situ* or from terrestrially derived sources, instead of new sources from *in situ* N_2 fixation . Finally, the spatial survey indicated that increases in AOA *amoA* and the AOA:β-AOB *amoA* ratio were associated with salinity, turbidity and ammonium concentrations, consistent with the higher AOA abundances observed in the ocean, hypothesized particle attachment or light inhibition, and niche partitioning. Also, this is one of the few surveys examining the relative AOA and β-AOB *amoA* abundance in an estuary that demonstrates that the AOA:β-AOB *amoA* ratio correlates positively with salinity - contrasting with some recent reports. However, the co-correlation of upwelled nutrient rich deep water, a phenomenon typical of Northeastern Pacific coastal systems, is a confounding factor and better temporal resolution is needed.

3.6 Experimental Procedures

3.6.1 *Sampling and Environmental Parameters*

Nine stations were sampled in the Columbia River, its estuary and the Willamette River from July 10-15, 2008 aboard the R/V *Clifford A. Barnes*. Temperature, pH, salinity, and transmissometry were measured using a Sea-Bird 911+CTD depth profiler (Sea-Bird Electronics Inc., Bellevue, WA). Dissolved oxygen (Sea-Bird) and chl *a* fluorescence (WetStar, Wetlabs, Inc.) sensors mounted on the CTD provided additional data. Due to the high current velocities of the system, water samples were obtained from surface (1m depth) and bottom (1m above bottom) waters with an *in situ* pump fastened to the CTD package which pumped sample water to the surface for collection. Samples for macro-

nutrient analyses (nitrate, nitrite, phosphate, silicate, and ammonium) were pre-filtered

through 25 mm diameter GF/F filters (Whatman International) and stored at -20˚C until

determined in the laboratory with a Astoria-Pacific Flow Analyzer system using standard

colorimetric methods (Parsons *et al.*, 1984). For molecular analyses of the prokaryotic

community, approximately 1 to 2 l of water was filtered through 0.22μm Sterivex filter

cartridges (Millipore Corp., Bedford, MA), preserved in 2 ml of RNAlater reagent

(Ambion, Austin, TX), frozen, and stored at -80˚C. The cartridges of the Sterivex filters

were cracked open and the filters and RNAlater reagent were transferred immediately for

DNA extraction using the FastDNA SPIN Kit for Soil (MP Biomedicals, Solon, OH)

with bead beading settings of 30 seconds at speed 5.5 with a FastPrep FP120 instrument

(MP Biomedicals, Solon, OH). DNA concentrations were quantified using a NanoDrop

ND-1000 spectrophotometer (NanoDrop Technologies, Wilmington, DE, USA).

From July 2009 to August 2010, monthly to semi-monthly water samples were

taken at a site in the lower Columbia River at mile marker 53 (46˚ 11' 4.20" N, -123˚ 11'

14.76" E) where a Land/Ocean Biogeochemical Observatory (LOBO) system is deployed

and taking hourly measurements of dissolved oxygen, salinity, temperature, turbidity,

chlorophyll, CDOM, and nitrate. Additionally, water samples were collected at the

surface and at 2.5m below the surface (at the depth of the LOBO sensors) with a Niskin

water sampler, and processed as mentioned above for discrete molecular analyses and

nutrient measurements.

3.6.2 *Quantitative PCR*

Quantitative PCR (qPCR) was used to estimate the number of archaeal and β-proteobacterial *amoA* copies, in the water samples collected at the 10 sites between July 2008 and June 2010. An iCycler real-time PCR system (Bio-Rad, Hercules, CA) was used to measure all samples, in triplicate or duplicate wells per reaction with all reactions performed, at least, in triplicate. Reactions were performed in a 25 μl volume with 1 μl of DNA template. All *amoA* qPCR assays used SYBRgreen reaction mixtures containing 12.5 μl iQ SYBR®Green Supermix (Bio-Rad) and either 400 nM or 300 nM primer concentrations for the archaeal and bacterial *amoA* assays, respectively. Bacterial *amoA* abundance was quantified using the *amoA* 1F/2R primer set (Rotthauwe *et al.*, 1997) with the following thermal profile: 3 min. at 95˚C, then 40 cycles consisting of 45 s at 94˚C, 30 s at 59˚C, 1 min. at 72˚C and a detection step for 15 s at 81˚C. Archaeal *amoA* abundance was quantified using primers Arch_amoA_F (de la Torre *et al.*, 2008) and Arch-amoA_R (Francis *et al.*, 2005) with the following thermal profile: 3 min. at 95˚C, then 36 cycles consisting of 30 s at 95˚C, 45 s at 56˚C, 1 min. at 72˚C and a detection step for 15 s at 81˚C.

Standard curves were generated for each primer set with serial dilutions of a standard containing a known number of the target sequences. Standards for archaeal and bacterial *amoA* were generated from PCR amplicons using the primer set and cycling conditions in Francis *et al*. (2005) and Rotthauwe *et al.* (1997), respectively. The PCR products were then purified using the Promega SV PCR Purification Kit (Promega) after visualization on an agarose gel, cloned using a TOPO TA cloning kit with TOP10 electrocompetent cells (Invitrogen, Carlsbad, CA), and subsequently sequenced to verify specificity. A PureYield™ Plasmid Mini-Prep system (Promega) was used to extract the

plasmids. Linearized plasmids were produced from cloned amplicons by digestion with

XbaI restriction enzyme (Promega), run on an agarose gel for visualization, and then

purified. DNA concentrations in the extracts were measured fluorometrically by

PicoGreen (Molecular Probes, Eugene, OR) staining on a NanoDrop ND-3300

Fluorospectrometer (NanoDrop). Gene abundance was calculated based on DNA

concentration and plasmid plus insert sequence size. Dilution series ranging from 10^0 to

10^5 copies μl^{-1} were used for the standard curves.

For bacterial *amoA,* standard curve correlation coefficients (R^2) averaged 0.991

(standard deviation of 0.011) and PCR efficiency averaged 92.1% (standard deviation of

9.1%). For archaeal *amoA*, standard curve correlation coefficients averaged 0.994

(standard deviation of 0.004) and PCR efficiency averaged 91% (standard deviation of

7%). Product specificity for all qPCR assays was verified by melt curve analysis and by

visualization in agarose gels of bands of the expected size. To counteract inhibitory

effects, serial dilutions of genomic DNA from representative samples were carried out

until amplification of the target product fell into a linear range and those dilutions would

then be used for all subsequent representative samples.

3.6.3 $\delta^{15}N$ in nitrate and nitrification rate measurements

Nitrification rate experiments using water collected at the SATURN-05 station

were carried out in August 2010, during a period of observed *in situ* NO_3^- increase

coincident with increased sky cover and precipitation thereby theoretically inactivating

phytoplankton NO_3^- uptake and allowing the *in situ* process of nitrification to be captured

by the continuous NO_3^- measurements. Bulk water samples were collected at dawn from

the surface depth of the water column and transported back to the laboratory for

immediate incubation. Experimental incubations were carried out in eight 250 ml bottles which were filled to a total volume of 315 ml each: two spiked with ^{15}N-labelled NH_4^+, two spiked with ^{15}N-labelled NO_3^-, and then two spiked with the nitrification inhibitor ATU along with ^{15}N-labelled NH_4^+ or ^{15}N-labelled NO_3^-. ^{15}N-labelled NH_4^+ and NO_3^- spikes were added to achieve spike concentrations of 53 nM NH_4^+ and 70 nM NO_3^-, respectively, while ATU spikes were added to achieve a final concentration of 75 μM. Bottles were incubated in the dark at a room temperature of ~22 ˚C (*in situ* water temperature at time of sample collection was ~21 ˚C) and 30 ml samples were removed from each bottle at time points of 0, 5.5, and 23 h (except for ATU spiked bottles, which were only sampled at 0 and 23 h), and stored at -20 ˚C until analysis for nutrients and $\delta^{15}N_{NO3}$. $\delta^{15}N_{NO3}$ values were obtained after cadmium reduction of sample NO_3^- using the sodium azide conversion of NO_2^- to N_2O (McIlvin and Altabet, 2005) and subsequent N_2O analysis in a PAL autosample/PreCon/GasBenchII assembly coupled to a Finnigan Delta^{PLUS} Advantage isotope ratio mass spectrometer. Uptake of ^{15}N into particulate matter was not measured in this experiment.

Nitrification rates, using ^{15}N-labelled NH_4^+ additions, were calculated by estimating the atom percent of ^{15}N in the NH_4^+ pool by mass balance from the t_0 NH_4^+ concentrations and the $^{15}NH_4^+$ additions, and then using a model similar to Montoya, *et al.* (1996). Nitrification rates, using ^{15}N-labelled NO_3^- additions, were determined from the magnitude of the dilution of added tracer, by determining isotopic enrichment and NO_3^- concentrations at t_0 and subsequent sampling points. Nitrification rates were then calculated according to the Blackburn-Caperon model (Clark *et al.*, 2007).

Natural abundance values of $\delta^{15}N$ in nitrate were determined using the denitrifier method of Sigman *et al* (2001) in the Stable Isotope Facility at the University of California at Davis. This method used the denitrifying bacteria *Pseudomonas chloroaphis*, which lack the enzyme to convert N_2O to N_2. After conversion of sample NO_2^- and NO_3^- to N_2O, trace gas isotope ratios were measured using a SerCon Cryoprep trace gas concentration system interface to a PDZ Europa 20-20 IRMS (Sercon Ltd., Cheshire, UK).

3.7 References

Aminot, A., Kirkwood, D. S. and Kérouel, R. (1997). Determination of ammonia in seawater by the indophenol-blue method: Evaluation of the ICES NUTS I/C 5 questionnaire. *Marine Chemistry* **56:** 59-75.

Beman, J. M., Popp, B. N. and Francis, C. A. (2008). Molecular and biogeochemical evidence for ammonia oxidation by marine Crenarchaeota in the Gulf of California. *ISME* **2:** 429-441.

Beman, J. M., Sachdeva, R. and Fuhrman, J. A. (2010). Population ecology of nitrifying archaea and bacteria in the Southern California Bight. *Environ. Microbiol* **12:** 1282-1292.

Bernhard, A. E., Landry, Z. C., Blevins, A., de la Torre, J. R., Giblin, A. E. and Stahl, D. A. (2010). Abundance of Ammonia-Oxidizing Archaea and Bacteria along an Estuarine Salinity Gradient in Relation to Potential Nitrification Rates. *Appl Environ Microbiol* **76:** 1285-1289.

Berounsky, V. M. and Nixon, S. W. (1993). Rates of Nitrification along an Estuarine Gradient in Narragansett Bay. *Estuaries* **16:** 718.

Billen, G. (1975). Nitrification in the Scheldt estuary (Belgium and the Netherlands). *Estuarine and Coastal Marine Science* **3:** 79-89.

Boatman, C. D. and Murray, J. W. (1982). Modeling Exchangeable NH4 + Adsorption in Marine Sediments: Process and Controls of Adsorption. *Limnology and Oceanography* **27:** 99-110.

Brion, N., Billen, G., Guézennec, L., Ficht, A., Guezennec, L. and Ficht, A. (2000). Distribution of Nitrifying Activity in the Seine River (France) from Paris to the Estuary. *Estuaries* **23:** 669-682.

Bru, D., Martin-Laurent, F. and Philippot, L. (2008). Quantification of the Detrimental Effect of a Single Primer-Template Mismatch by Real-Time PCR Using the 16S rRNA Gene as an Example. *Appl Environ Microbiol* **74:** 1660-1663.

Bruland, K. W., Lohan, M. C., Aguilar-Islas, A. M., Smith, G. J., Sohst, B. and Baptista, A. (2008). Factors influencing the chemistry of the near-field Columbia River plume: Nitrate, silicic acid, dissolved Fe, and dissolved Mn. *Journal of Geophysical Research (Oceans)* **113**.

Caffrey, J. M., Bano, N., Kalanetra, K. and Hollibaugh, J. T. (2007). Ammonia oxidation and ammonia-oxidizing bacteria and archaea from estuaries with differing histories of hypoxia. *ISME* **1:** 660-662.

Carpenter, K.D. and Waite, I.R. (2000) Relations of habitat specific algal assemblages to land use and water chemistry in the Willamette basin, Oregon. *Environmental Monitoring and Assessment* **64:** 247–257.

Casciotti, K. L., Sigman, D. M. and Ward, B. B. (2002). Linking Diversity and Stable
  Isotope Fractionation in Ammonia-Oxidizing Bacteria. *Geomicrobiology Journal*,
  20: 335-353.

Cébron, A., Berthe, T. and Garnier, J. (2003). Nitrification and Nitrifying Bacteria in the
  Lower Seine River and Estuary (France). *Appl Environ Microbiol* **69:** 7091-7100.

Church, M. J., Wai, B., Karl, D. M. and DeLong, E. F. (2010). Abundances of
  crenarchaeal amoA genes and transcripts in the Pacific Ocean. *Environ Microbiol*
  12: 679-688.

Clark, D. R., Rees, A. P. and Joint, I. (2007). A method for the determination of
  nitrification rates in oligotrophic marine seawater by gas chromatography/mass
  spectrometry. *Marine Chemistry* **103:** 84-96.

Clark, D. R., Rees, A. P. and Joint, I. (2008). Ammonium regeneration and nitrification
  rates in the oligotrophic Atlantic Ocean: Implications for new production
  estimates. *Limnol. Oceangr.* **53:** 52-62.

Colbert, D. and McManus, J. (2003). Nutrient Biogeochemistry in an Upwelling-
  Influenced Estuary of the Pacific Northwest (Tillamook Bay, Oregon, USA).
  Estuaries **26:** 1205-1219.

Crump , B.C. and Baross, J.A. (1996). Particle-attached bacteria and heterotrophic
  plankton associated with the Columbia River estuarine turbidity maxima. *Mar
  Ecol Prog Ser* **138:** 265-273.

Crump, B.C. and Baross, J.A. (2000). Archaeaplankton in the Columbia River, its estuary
  and the adjacent coastal ocean, USA. *FEMS Microbiol. Ecol* **31:** 231-239.

Daum, M., Zimmer, W., Papen, H., Kloos, K., Nawrath, K. and Bothe, H. (1998).

Physiological and molecular biological characterization of ammonia oxidation of the heterotrophic nitrifier Pseudomonas putida. *Curr. Microbiol* **37:** 281-288.

Feliatra, F. and Bianchi, M. (1993). Rates of nitrification and carbon uptake in the Rhone River plume (northwestern Mediterranean Sea). *Microb Ecol* **26:** 21-28.

Francis, C. A., Roberts, K. J., Beman, J. M., Santoro, A. E. and Oakley, B. B. (2005). Ubiquity and diversity of ammonia-oxidizing archaea in water columns and sediments of the ocean. *Proceedings of the National Academy of Science* **102:** 14683-14688.

Galloway, J. N., and Cowling, E. B. (2002). Reactive Nitrogen and the World: 200 Years of Change. *Ambio* **31:** 64-71.

Hales, B., Karp-Boss, L., Perlin, A., and Wheeler, P. A. (2006). Oxygen production and carbon sequestration in an upwelling coastal margin. *Global Biogeochemical Cycles* **20**.

Hatzenpichler, R., Lebedeva, E. V., Spieck, E., Stoecker, K., Richter, A., Daims, H. and Wagner, M. (2008). A moderately thermophilic ammonia-oxidizing crenarchaeote from a hot spring. *Proceedings of the National Academy of Science* **105:** 2134-2139.

He, J., Shen, J., Zhang, L., Zhu, Y., Zheng, Y., Xu, M. and Di, H. (2007). Quantitative analyses of the abundance and composition of ammonia-oxidizing bacteria and ammonia-oxidizing archaea of a Chinese upland red soil under long-term fertilization practices. *Environ. Microbiol* **9:** 2364-2374.

Herfort, L., Kim, J., Coolen, M. J. L., Abbas, B., Schouten, S., Herndl, G. J. and Damste, J. S. S. (2009). Diversity of Archaea and detection of crenarchaeotal amoA genes

in the rivers Rhine and Têt. *Aquat Microb Ecol* **55:** 189-201.

Holmes, R. M., Aminot, A., Kérouel, R., Hooker, B. A. and Peterson, B. J. (1999). A simple and precise method for measuring ammonium in marine and freshwater ecosystems. *Can. J. Fish. Aquat. Sci.* **56:** 1801-1808.

Horrigan, S. G. and Springer, A. L. (1990). Oceanic and Estuarine Ammonium Oxidation: Effects of Light. *Limnology and Oceanography* **35:** 479-482.

Jay, D. A., Giese, B. S. and Sherwood, C. R. (1990). Energetics and sedimentary processes in the Columbia River Estuary. *Progress In Oceanography* **25:** 157-174.

Jia, Z. and Conrad, R. (2009). Bacteria rather than Archaea dominate microbial ammonia oxidation in an agricultural soil. *Environ. Microbiol* **11:** 1658-1671.

Kaplan, W. (1983). Nitrification, p. 139-190. In E. Carpenter(ed.), Nitrogen in the marine environment. Academic Press, New York.

Kiefer, D., Olson, R. and Holm-Hansen, O. (1976). Another look at the nitrite and chlorophyll maxima in the central North Pacific. *Deep Sea Research and Oceanographic Abstracts* **23:** 1199-1208.

Leininger, S., Urich, T., Schloter, M., Schwark, L., Qi, J., Nicol, G. W., Prosser, J. I., Schuster, S. C. and Schleper, C. (2006). Archaea predominate among ammonia-oxidizing prokaryotes in soils. *Nature* **442:** 806-809.

Limpiyakorn, T., Shinohara, Y., Kurisu, F. and Yagi, O. (2005). Communities of ammonia-oxidizing bacteria in activated sludge of various sewage treatment plants in Tokyo. *FEMS Microbiology Ecology* **54:** 205-217.

Lipschultz, F., Wofsy, S. C. and Fox, L. E. (1985). The effects of light and nutrients on

rates of ammonium transformation in a eutrophic river. *Marine Chemistry* **16:**
329-341.

Lipschultz, F., Wofsy, S. C. and Fox, L. E. (1986). Nitrogen Metabolism of the Eutrophic
Delaware River Ecosystem. *Limnology and Oceanography* **31:** 701-716.

Liu, Z., Huang, S., Sun, G., Xu, Z. and Xu, M. (2010). Diversity and abundance of
ammonia-oxidizing archaea in the Dongjiang River, China. *Microbiol Res*.

Lomas, M. W. and Glibert, P. M. (1999). Temperature Regulation of Nitrate Uptake: A
Novel Hypothesis about Nitrate Uptake and Reduction in Cool-Water Diatoms.
Limnology and Oceanography **44:** 556-572.

Lomas, M. W. and Glibert, P. M. (2000). Comparisons of nitrate uptake, storage, and
reduction in marine diatoms and flagellates. *J Phycol* **36:** 903-913.

Norton, J.M*., Alzerreca, J.J., Suwa, Y., and Klotz, M.G. (*2002*) Diversity of ammonia
monooxygenase operon in autotrophic ammonia-oxidizing bacteria. Arch
Microbiol* **177***: 139–149*.

Lomas, M. W. and Lipschultz, F. (2006). Forming the Primary Nitrite Maximum:
Nitrifiers or Phytoplankton? *Limnology and Oceanography* **51:** 2453-2467.

Martens-Habbena, W., Berube, P. M., Urakawa, H., de la Torre, J. R. and Stahl, D. A.
(2009). Ammonia oxidation kinetics determine niche separation of nitrifying
Archaea and Bacteria. *Nature* **461:** 976-979.

McCarthy, J. J., Kaplan, W. and Nevins, J. L. (1984). Chesapeake Bay Nutrient and
Plankton Dynamics. 2. Sources and Sinks of Nitrite. *Limnology and
Oceanography* **29:** 84-98.

McIlvin, M. R. and Altabet, M. A. (2005). Chemical conversion of nitrate and nitrite to

nitrous oxide for nitrogen and oxygen isotopic analysis in freshwater and seawater. *Anal. Chem* **77:** 5589-5595.

Mincer, T. J., Church, M. J., Taylor, L. T., Preston, C., Karl, D. M. and DeLong, E. F. (2007). Quantitative distribution of presumptive archaeal and bacterial nitrifiers in Monterey Bay and the North Pacific Subtropical Gyre. *Environ. Microbiol* **9:** 1162-1175.

Moin, N. S., Nelson, K. A., Bush, A. and Bernhard, A. E. (2009). Distribution and Diversity of Archaeal and Bacterial Ammonia Oxidizers in Salt Marsh Sediments. *Appl Environ Microbiol* **75:** 7461-7468.

Montoya, J. P., Voss, M., Kahler, P. and Capone, D. G. (1996). A Simple, High-Precision, High-Sensitivity Tracer Assay for N(inf2) Fixation. *Appl Environ Microbiol* **62:** 986-993.

Mosier, A. C. and Francis, C. A. (2008). Relative abundance and diversity of ammonia-oxidizing archaea and bacteria in the San Francisco Bay estuary. *Environ. Microbiol* **10:** 3002-3016.

Nicol, G. W., Leininger, S., Schleper, C. and Prosser, J. I. (2008). The influence of soil pH on the diversity, abundance and transcriptional activity of ammonia oxidizing archaea and bacteria. *Environ. Microbiol* **10:** 2966-2978.

Olson, R. J., Soohoo, J. B. and Kiefer, D. A. (1980). Steady-state Growth of the Marine Diatom Thalassiosira pseudonana: Uncoupled kinetics of nitrate uptake and nitrite production. *Plant Physiol.* **66:** 383-389.

Olson, R.J. *(*1981*)* Differential photoinhibition of marine nitrifying bacteria: a possible mechanism for the formation of the primary nitrite maximum. *J Mar Res* **39***:* 227–

238.

Owens, N. (1986). Estuarine nitrification: A naturally occurring fluidized bed reaction? *Estuarine Coastal and Shelf Science* **22:** 31-44.

Papen, H., von Berg, R., Hinkel, I., Thoene, B. and Rennenberg, H. (1989). Heterotrophic nitrification by Alcaligenes faecalis: NO2-, NO3-, N2O, and NO production in exponentially growing cultures. *Appl Environ Microbiol* **55:** 2068-2072.

Parsons, T. R., Maita, Y. and Lalli, C. M. (1984). *A manual of chemical and biological methods for seawater analysis / by Timothy R. Parsons, Yoshiaki Maita and Carol M. Lalli.* , Pergamon international library of science, technology, engineering, and social studies. Oxford [Oxfordshire]; New York :: Pergamon Press.

Pedersen, H., Dunkin, K. A. and Firestone, M. K. (1999). The relative importance of autotrophic and heterotrophic nitrification in a conifer forest soil as measured by15N tracer and pool dilution techniques. *Biogeochemistry* **44:** 135-150.

Peterson, C., Scheidegger, K., Komar, P. and Niem, W. (1984). Sediment composition and hydrography in six high-gradient estuaries of the northwestern United States. *Journal of Sedimentary Research* **54:** 86-97.

Plummer, D. H., Owens, N. J. P. and Herbert, R. A. (1987). Bacteria—particle interactions in turbid estuarine environments. *Continental Shelf Research* **7:** 1429-1433.

Rabalais, N. N. (2002). Nitrogen in aquatic ecosystems. *Ambio* **31:** 102-112.

Reed, D.J. and Donovan, J. (1994) The character and composition of the Columbia River estuarine turbidity maximum. In: K. R. Dyer and R. J. Orth, Editors, *Changes in Fluxes in Estuaries: Implications from Science to Management*, Olsen and Olsen,

Fredensborg , pp. 445–450.

Rotthauwe, J. H., Witzel, K. P. and Liesack, W. (1997). The ammonia monooxygenase structural gene amoA as a functional marker: molecular fine-scale analysis of natural ammonia-oxidizing populations. *Appl Environ Microbiol* **63:** 4704-4712.

Santoro, A. E., Francis, C. A., de Sieyes, N. R. and Boehm, A. B. (2008). Shifts in the relative abundance of ammonia-oxidizing bacteria and archaea across physicochemical gradients in a subterranean estuary. *Environ. Microbiol* **10:** 1068-1079.

Santoro, A.E., Casciotti, K.L., and Francis, C.A. (2010). Activity, abundance and diversity of nitrifying archaea and bacteria in the central California Current. *Environ. Microbiol.* **12:** 1989-2006.

Schimel, J. P., Firestone, M. K. and Killham, K. S. (1984). Identification of Heterotrophic Nitrification in a Sierran Forest Soil. *Appl Environ Microbiol* **48:** 802-806.

Seitzinger, S., Harrison, J. A., Böhlke, J. K., Bouwman, A. F., Lowrance, R., Peterson, B., Tobias, C., and Drecht, G.V. (2006). Denitrification across landscapes and waterscapes: a synthesis. *Ecological Applications* **16:** 2064-2090.

Shen, J., Zhang, L., Zhu, Y., Zhang, J. and He, J. (2008). Abundance and composition of ammonia-oxidizing bacteria and ammonia-oxidizing archaea communities of an alkaline sandy loam. *Environ. Microbiol* **10:** 1601-1611.

Sigleo, A. C. and Frick, W. E. (2007). Seasonal variations in river discharge and nutrient export to a Northeastern Pacific estuary. *Estuarine Coastal and Shelf Science* **73:** 368-378.

Sigman, D. M., Casciotti, K. L., Andreani, M., Barford, C., Galanter, M. and Böhlke, J.

K. (2001). A bacterial method for the nitrogen isotopic analysis of nitrate in seawater and freshwater. *Anal. Chem* **73:** 4145-4153.

Sigman, D.M. and Casciotti, K.L. (2009) Nitrogen isotopes in the ocean. In: J.H. Steele, K.K. Turekian and S.A. Thorpe, Editors, *Encyclopedia of Ocean Sciences*, Academic Press, London, pp. 1884–1894.

de la Torre, J. R., Walker, C. B., Ingalls, A. E., Könneke, M. and Stahl, D. A. (2008). Cultivation of a thermophilic ammonia oxidizing archaeon synthesizing crenarchaeol. *Environ. Microbiol* **10:** 810-818.

Vaccaro, R. F. and Ryther, J. H. (1960). Marine Phytoplankton and the Distribution of Nitrite in the Sea. *Journal du Conseil* **25:** 260 -271.

Vincent, W., Chang, F., Cole, A., Downes, M., James, M., May, L., Moore, M. and Woods, P. (1989). Short-term changes in planktonic community structure and nitrogen transfers in a coastal upwelling system. *Estuarine Coastal and Shelf Science* **29:** 131-150.

Vitousek, P. M., Aber, J. D., Howarth, R. W., Likens, G. E., Matson, P. A., Schindler, D. W., Schlesinger, W. H. and Tilman, D. G. (1997). Technical Report: Human Alteration of the Global Nitrogen Cycle: Sources and Consequences. *Ecological Applications* **7:** 737-750.

Wagner, M., Rath, G., Amann, R., Koops, H.-P., and Schleifer, K.-H.. (1995). *In situ* identification of ammonia-oxidizing bacteria. *Syst. Appl. Microbiol.* **1:** 251-264.

Wang, H., Shen, Z., Niu, J., He, Y., Hong, Q. and Wang, Y. (2010). Functional bacteria as potential indicators of water quality in Three Gorges Reservoir, China. *Environ Monit Assess* **163:** 607-617.

Ward, B. (1987). Nitrogen transformations in the Southern California Bight. *Deep Sea Research Part I: Oceanographic Research* **34:** 785-805.

Ward, B. B. and O'Mullan, G. D. (2002). Worldwide Distribution of Nitrosococcus oceani, a Marine Ammonia-Oxidizing γ-Proteobacterium, Detected by PCR and Sequencing of 16S rRNA and amoA Genes. *Appl Environ Microbiol* **68:** 4153-4157.

Wells, G. F., Park, H., Yeung, C., Eggleston, B., Francis, C. A. and Criddle, C. S. (2009). Ammonia-oxidizing communities in a highly aerated full-scale activated sludge bioreactor: betaproteobacterial dynamics and low relative abundance of Crenarchaea. *Environ. Microbiol* **11:** 2310-2328.

Wetz, M. S., Hales, B., Chase, Z., Wheeler, P. A., and Whitney, M. M. (2006). Riverine Input of Macronutrients, Iron, and Organic Matter to the Coastal Ocean off Oregon, U.S.A., during the Winter. *Limnology and Oceanography* **51**: 2221-2231.

Wuchter, C., Abbas, B., Coolen, M.J., Herfort, L., van Bleijswijk, J., Timmers, P., *et al*. (2006). Archaeal nitrification in the ocean **103:** 12317-12322.

Xia, X., Yang, Z. and Zhang, X. (2009). Effect of suspended-sediment concentration on nitrification in river water: importance of suspended sediment-water interface. *Environ. Sci. Technol* **43:** 3681-3687.

3.8 Figures and Tables

Figure 3.1 Location of sampling sites within the lower Columbia River and Estuary. Sites representing different hydrodynamic regimes are color coded: Columbia River Estuary – teal; Lower Columbia River – green; SATURN-05 site on the Lower CR – yellow; Willamette River – red.

Station	Hydro-dynamic region	Longitude	Date(s) sampled	Depths	Variables
A	Columbia River estuary	-123.96	July 10, 2008	Bottom (1 m above bottom) Surface (0.5 m)	AOA *amoA*, β-AOB *amoA*, NH_4^+, NO_2^-, NO_3^-, PO_4^-, SiO_4^-; CTD: salinity, depth, temperature, DO, light transmissivity chlorophyll,
B		-123.86	July 11, 2008		
C		-123.73	July 11-12, 2008		
D		-123.68	July 12-13, 2008		
E	Lower Columbia River	-123.37	July 14, 2008		
F		-123.01	July 14, 2008		
G		-122.95	July 15, 2008		
H	Willamette River	-122.75	July 15, 2008		
I		-122.67	July 15, 2008		
SATURN-05	Lower Columbia River	-123.11	July 2009 – August 2010	Surface 2.5 m	AOA *amoA*, β-AOB *amoA*, $\delta^{15}NO_3^-$, NH_4^+, NO_2^-, NO_3^-, PO_4^-, SiO_4^-; *in situ*: NO_3^-, chlorophyll, DO, pressure, temperature

Table 3.1 Location and time of sampling points, along with variables analyzed in this study.
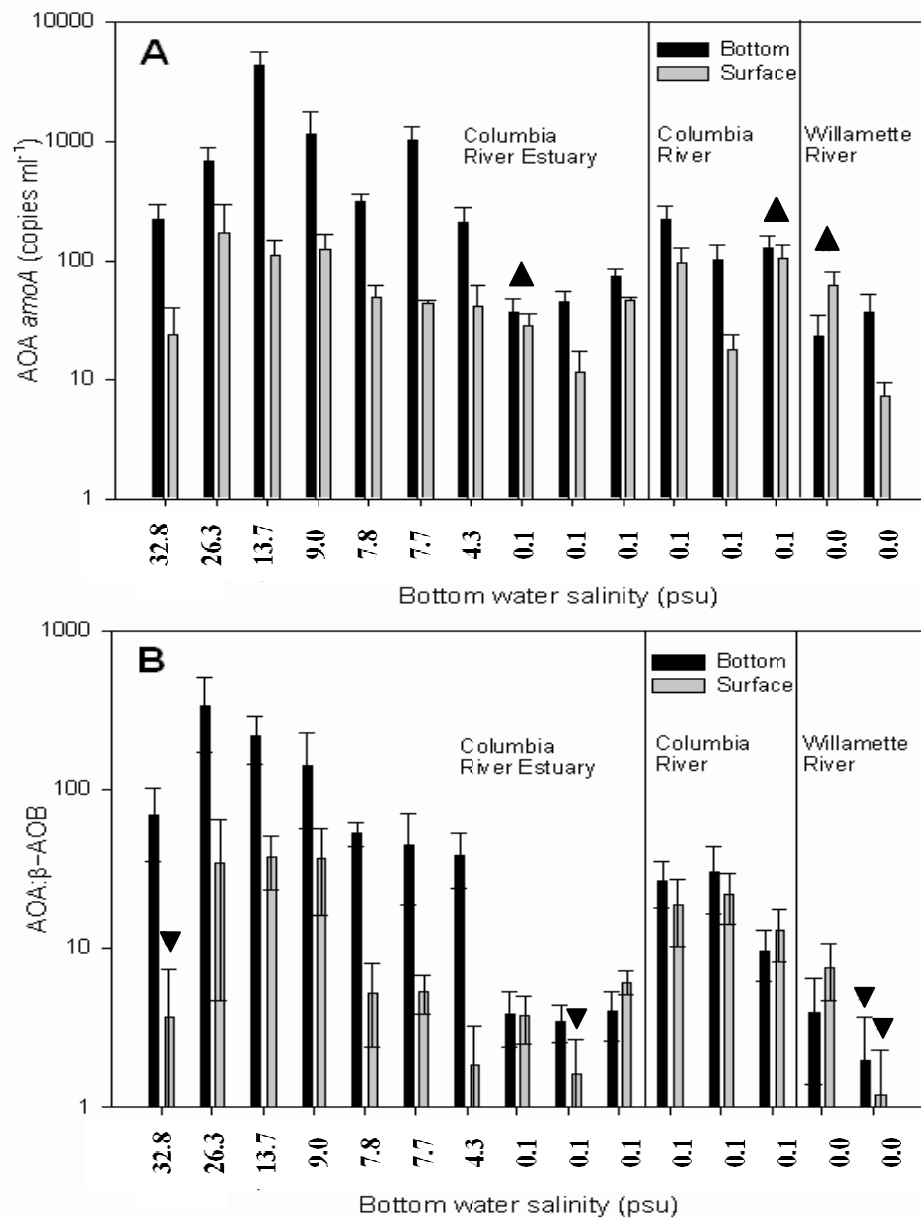
Figure 3.2 AOA *amoA* copy numbers (a) and the AOA:β-AOB *amoA* ratio (b) in the Columbia River System water column as determined by quantitative PCR. Bottom and surface water column values were plotted against bottom water salinity to highlight its influence. ▲in (a) indicate sampling casts where bottom and surface water did not display a significant difference (student's t-test, $p < 0.05$); all other points were significantly different. ▼in (b) indicate individual samples where AOA *amoA* were not significantly different from β-AOB *amoA*, i.e. AOA: β-AOB *amoA* is < 1 (student's t-test, $p < 0.05$); all other points were significantly different. Error bars denote one standard deviation of at least triplicate qPCR measurements.

Station	Cast	Sample	Longitude	Depth	β-AOB amoA (copies/mL)	Salinity (psu)	NH$_4^+$ (μM)	Nitrate (μM)	Nitrite (μM)	Phosphate (μM)	Oxygen (μM)	Chlorophyll a (μg/L)	Light Transm. (%)
A	7	B008	-123.96	Bottom	3 ± 1	32.8	0.4	29.1	0.21	1.92	2.32	0.06	66.13
A	7	B010	-123.96	Surface	6 ± 4	1.5	NA	NA	NA	0.20	9.29	1.72	53.65
A	19	B015	-123.96	Bottom	20 ± 3	13.7	3.0	14.0	0.4	1.15	6.78	0.47	19.07
A	19	B017	-123.96	Surface	3 ± 0.6	1.2	0.7	1.3	0.14	0.29	9.35	1.51	51.76
B	32	B033	-123.86	Bottom	2 ± 1	26.3	4.1	26.5	0.34	1.60	3.90	0.57	48.96
B	32	B035	-123.86	Surface	5 ± 2	0.6	0.2	2.0	0.41	0.26	9.67	1.94	46.82
C	30	B027	-123.73	Bottom	5 ± 1	4.3	2.9	5.4	0.15	0.51	8.35	1.18	54.91
C	30	B029	-123.73	Surface	22 ± 12	0.05	0.1	14.0	0.17	0.30	9.69	1.84	55.41
C	52	B048	-123.73	Bottom	8 ± 2	9.0	5.2	9.8	0.40	0.65	7.49	0.73	57.14
C	52	B050	-123.73	Surface	3 ± 2	0.06	NA	6.7	0.13	0.07	10.56	1.95	43.16
D	51	B045	-123.68	Bottom	19 ± 8	0.05	1.2	1.7	0.26	0.05	10.08	2.30	49.70
D	51	B047	-123.68	Surface	7 ± 2	0.05	0.6	1.5	0.33	0.22	10.20	2.59	51.72
D	65	B054	-123.66	Bottom	13 ± 3	0.05	1.0	0.6	0.05	0.12	10.23	2.46	49.53
D	65	B056	-123.66	Surface	7 ± 3	0.05	0.8	1.8	0.08	0.12	10.19	2.46	50.73
D	68	B060	-123.66	Bottom	6 ± 0.4	7.8	0.8	8.5	0.22	0.27	7.71	1.42	54.65
D	68	B062	-123.66	Surface	9 ± 5	0.06	0.7	2.1	0.25	0.09	10.14	2.43	52.11
D	75	B067	-123.68	Bottom	10 ± 3	0.08	0.8	1.5	0.2	0.09	10.01	2.24	48.55
D	75	B069	-123.68	Surface	7 ± 2	0.06	0.6	1.0	0.14	0.07	10.37	1.77	50.34
D	76	B070	-123.69	Bottom	23 ± 12	7.7	4.5	5.9	0.43	0.43	7.89	1.48	46.60
D	76	B072	-123.69	Surface	8 ± 4	0.06	NA	NA	NA	0.04	10.33	0.65	49.82
E	96	B093	-123.37	Bottom	13 ± 3	0.05	0.6	1.9	0.22	0.09	9.79	2.52	44.76
E	96	B095	-123.37	Surface	8 ± 2	0.05	0.4	2.0	0.48	0.23	10.02	1.97	48.33
F	100	B101	-123.01	Bottom	3 ± 1	0.05	0.3	2.0	0.21	0.20	10.10	2.42	42.96
F	100	B102	-123.01	Surface	1 ± 0.1	0.05	NA	NA	NA	0.21	10.08	2.62	45.04
G	101	B103	-122.95	Bottom	8 ± 1	0.05	0.4	2.1	0.24	0.14	9.88	2.22	46.52
G	101	B104	-122.95	Surface	5 ± 2	0.05	0.6	2.4	0.18	0.17	9.87	1.99	46.62
H	103	B107	-122.75	Bottom	19 ± 13	0.04	4.5	14.3	0.91	0.64	7.81	0.54	38.47
H	103	B108	-122.75	Surface	6 ± 5	0.04	1.8	13.5	0.73	0.56	9.35	2.18	43.86
I	104	B109	-122.67	Bottom	6 ± 2	0.04	5.9	16.2	0.90	0.99	8.17	0.48	48.11
I	104	B110	-122.67	Surface	8 ± 2	0.04	4.5	15.8	0.77	0.86	8.67	0.76	54.58

Table 3.2 Physical and chemical properties of Columbia River System water column samples as listed longitudinally (1st) and in order of sampling (2nd). NA stands for 'not available'.

CCA variable scores
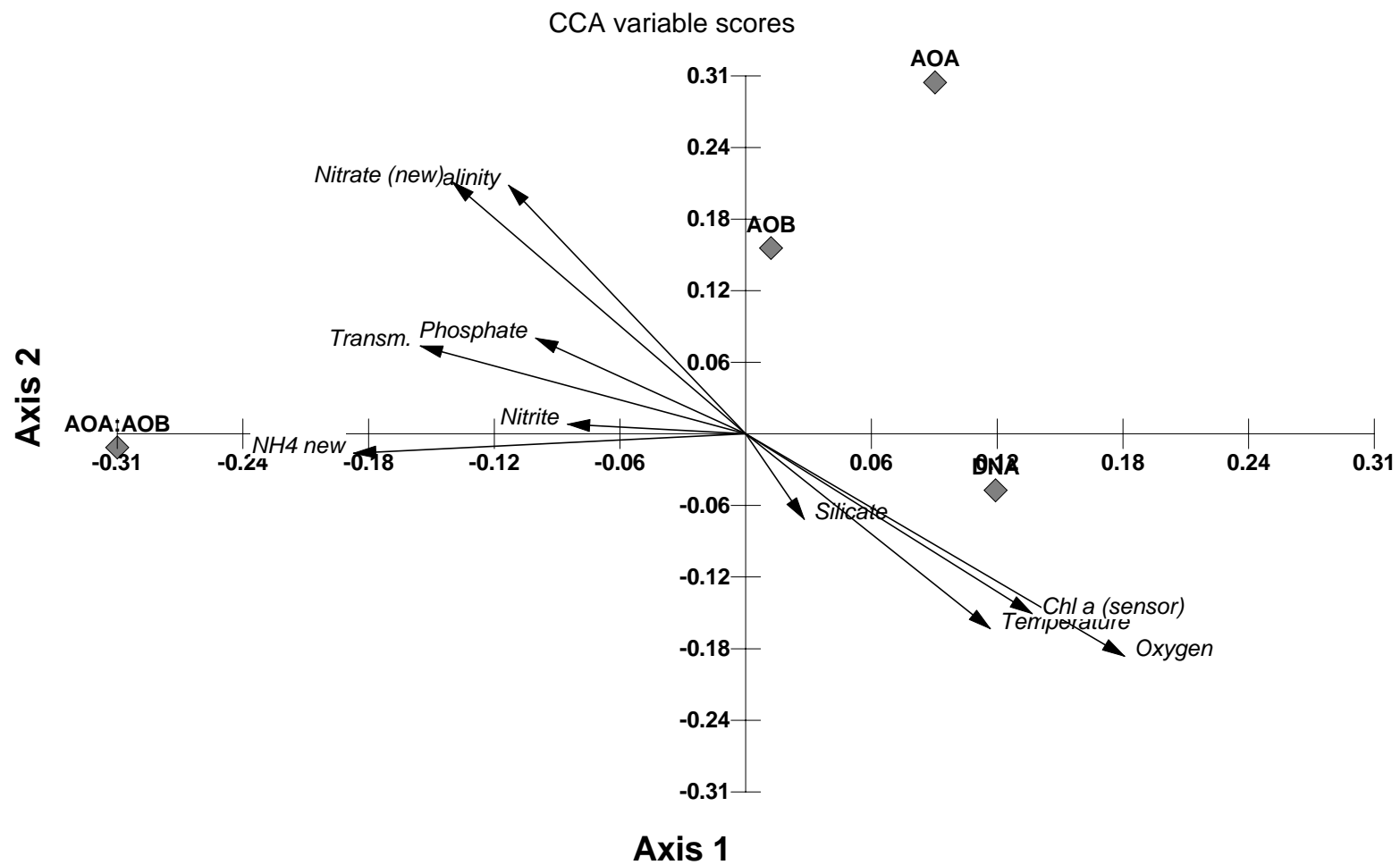
Figure 3.3 Canonical correspondence analysis of AOA *amoA* gene abundance, β-AOB *amoA* gene abundance, the AOA:β-AOB *amoA* ratio, DNA concentrations and environmental variables from Columbia River System water column samples.

Figure 3.4 (see next page)
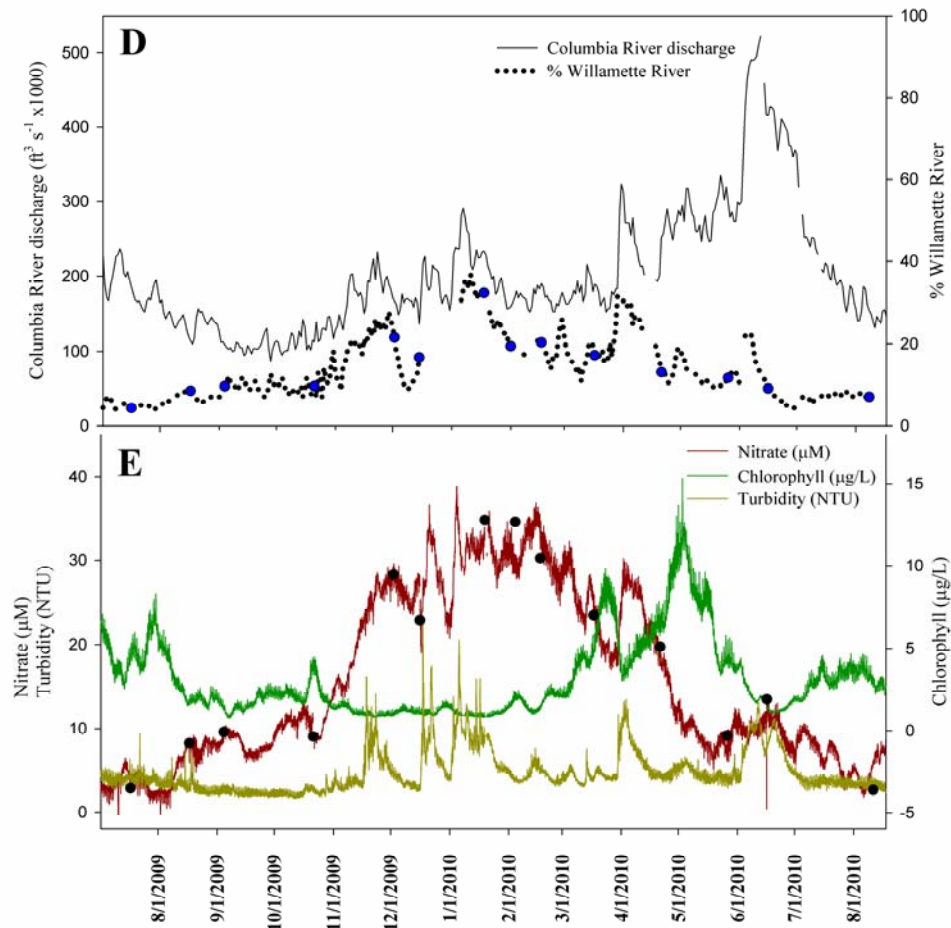
Figure 3.4 (continued) Ecological dynamics of nitrification at SATURN-05. Time series from July 2009 to August 2010 show measurements of: (a) AOA *amoA* gene copies (black) and β-AOB *amoA* gene copies (gray) with black and gray arrows in upward or downward directions signifying significant differences (student's t-test, $p < 0.05$) in indicated direction when compared to the previous time point; (b) NH_4^+ (●)and NO_2^- (○) concentrations; (c) NO_3^- concentrations and $\delta^{15}N\text{-}NO_3^-$ values (‰); (d) Columbia River discharge at SATURN-05 LOBO and the percent contribution of the Willamette River; (e) Nitrate (red), chlorophyll (green), and turbidity (yellow) concentrations as measured *in situ*. Gray boxes encompassing (a), (b), and (c) highlight points of interest. Dots in (d) and (e) indicate discrete sampling points and in (e) reflect nutrient measurements obtained from the laboratory. Error bars in (a) reflect one standard deviation qPCR measurements performed at the least in triplicate and the average of surface and 3m water column samples.

96
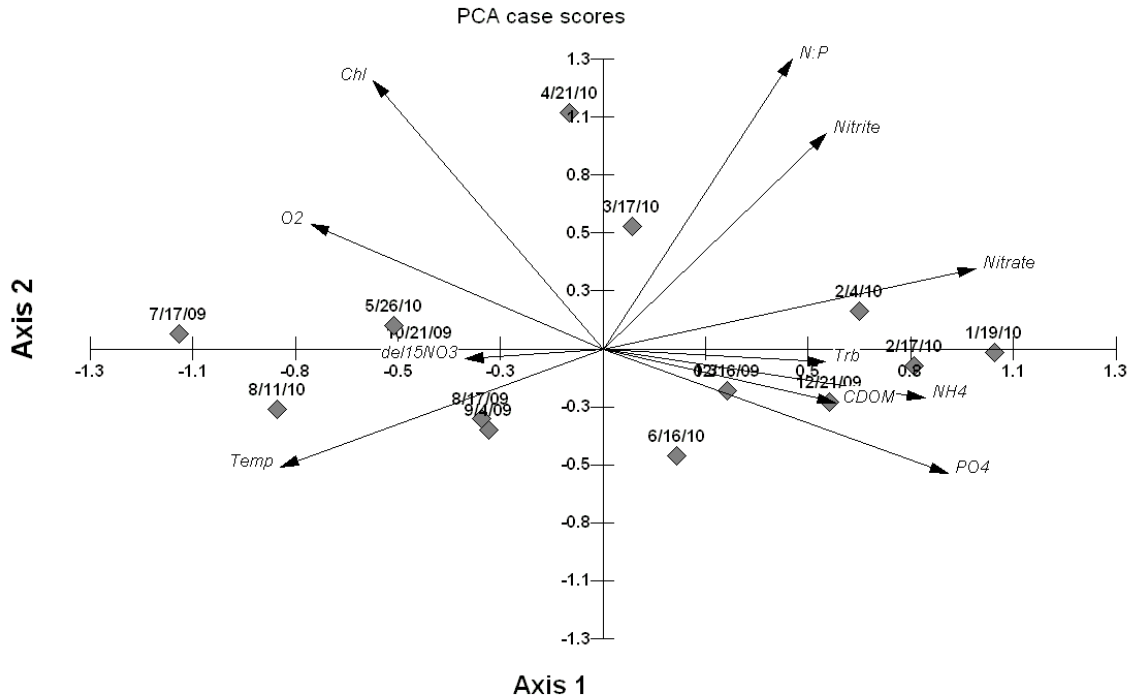
Figure 3.5 Principal component analysis of environmental variables from monthly water column samples at SATURN-05.

$$y = 0.0077x^2 - 0.4011x + 8.0623$$
$$R^2 = 0.6145$$
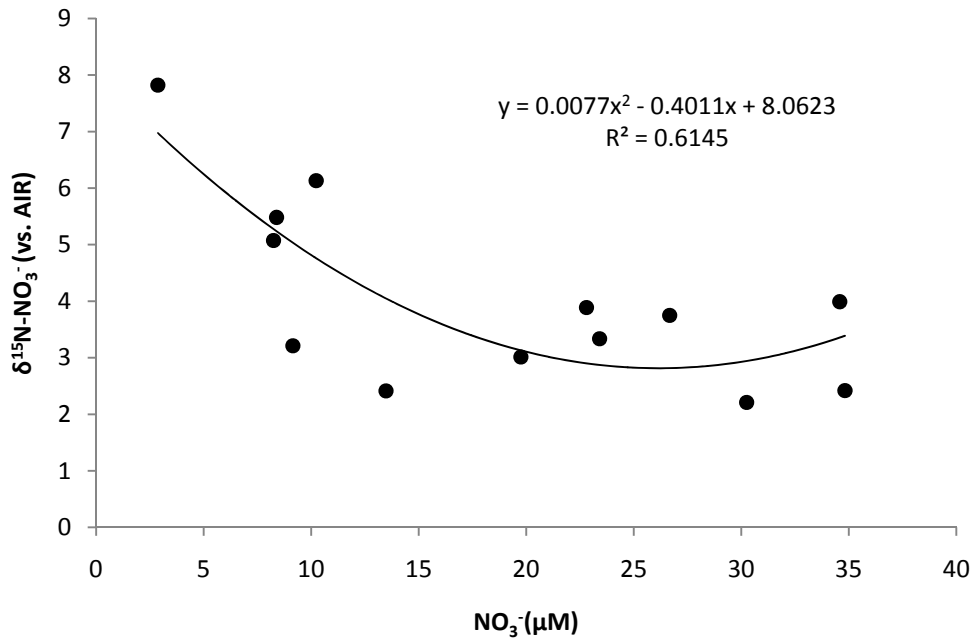
Figure 3.6 $\delta^{15}N$ values of riverine nitrate versus NO_3^- concentrations. A 2nd degree polynomial regression yielded a positive relation with a r^2 value of 0.61. A Pearson correlation was found to be significant with an r value of 0.66 (p < 0.05).

Figure 3.7 Nitrification rate measurements derived using $^{15}NH_4^+$ tracer and $^{15}NO_3^-$ pool dilution techniques, and allylthiourea additions (ATU) in unfiltered river water in August 2010. Inset shows concurrent *in situ* biogeochemical measurements of nitrate and chlorophyll, with nitrate displaying an apparent increase of approximately 800 nm d^{-1} over a 4-day period. Samples for nitrification incubation experiments were taken before sunrise on August 11, 2010 and incubated for approximately 23 hours.
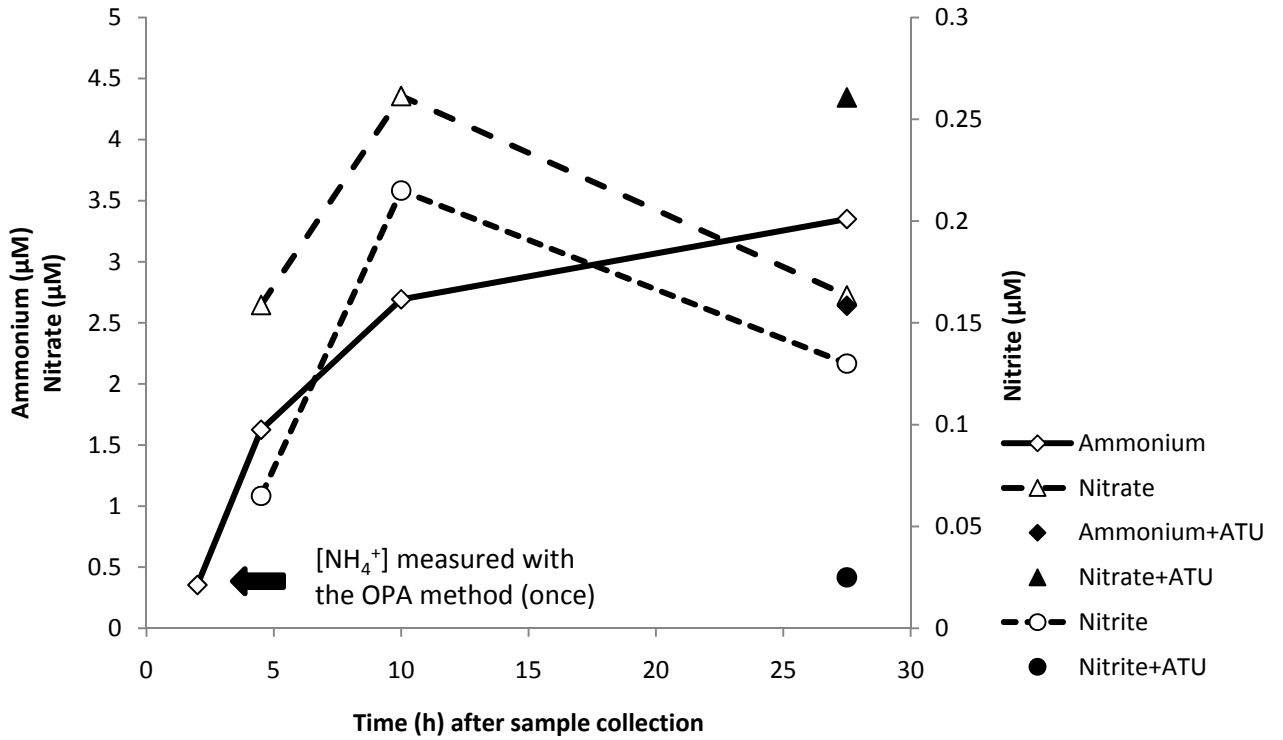
Figure 3.8 Nitrogen species dynamics in nitrification incubation experiment. First ammonium measurement was conducted using the fluorometric OPA method, with subsequent measurements made with the indophenol blue method. Filled symbols at the end of the experiment reflect nutrient concentrations in incubation bottles amended with allylthiourea (ATU).

CHAPTER 4

Final Considerations

4.1 Synthesis and Conclusions

The work presented in the preceding chapters were attempts at elucidating the fixed Nr

cycle in the Columbia River system (CRS) as well as enhancing an analytical method for

the measurement of ammonium, a critical constituent in the Nr cycle. Specifically,

attempts were focused on nitrification, a process that recycles Nr but also makes it

available for denitrification. Since both of these microbially-driven processes are crucial

to Nr cycling and can have varying levels of relative influence depending on the spatial

compartment (i.e. terrestrial, river, estuaries, etc.) and temporal sensitivities, spatial and

temporal surveys were carried out to investigate the importance of nitrification in the

lower Columbia River ecosystem. Q-PCR was used to assay the genetic potential for

ammonia oxidation (*amoA* genes) within the microbial population in the CRS between

two groups of ammonia oxidizers, the ammonia-oxidizing archaea (AOA) and ammonia-

oxidizing bacteria in the betaproteobacterial subdivision (β-AOB). In the temporal

survey, chemical sensor time series data, discrete chemical measurements, and ^{15}N

natural abundance and tracer stable isotope studies accompanied the ammonia-oxidizer

community measurements.

The improvement of the fluorometric method for the measurement of ammonium was achieved by using standard additions of ammonium and DOC in concert with spectrofluorometry in order to correct for the absorptive properties of DOC. This corrective action can be easily applied and adapted to *in situ* sensors, where high and fluctuating DOC concentrations are a concern, since the correction allows for the possibility to generate very similar standard curves among samples with varying DOC concentrations. This absorption correction, known commonly as the inner filter effect (IFE) correction, removed most of the interferences associated with DOC and allowed for more accurate determinations of ammonium concentrations in natural waters with DOC concentrations as low as 6.25 mg/L. The CR and CRE systems do not typically experience such high concentrations although some instances – as captured by discrete sampling - come quite close. However, the Willamette River and its smaller tributaries, routinely experience higher DOC concentrations than the CR, with concentrations extending into the 6.25 mg/L range. Numerous major world rivers, particularly in the wet tropics and even in the taiga, experience mean DOC concentrations around 8 mg/L and peak discharge DOC concentrations as high as 25 mg/L. Also, Blackwater rivers and wetlands in North America can typically reach or exceed the maximum 52.47 mg/L DOC value used in the study.

The temporal survey of nitrification is the most extensive record of AOA and β-AOB community dynamics in a large river to date. Several interesting correlations and tandem fluctuations were observed between the AOA:β-AOB *amoA* ratio and environmental variables, including ammonium, nitrite, δ^{15}N in nitrate, and discharge. These relationships indicate a prospectively large role of AOA in mesotrophic river

nitrification, and a demonstrated niche partitioning of AOA and β-AOB associated directly with substrate availability as an indirect result of river discharge and watershed land-use factors. Additionally, episodic variations in *in situ* nitrate were associated with high discharge events, turbidity, and chlorophyll concentrations, with the former two variables causing high nitrate concentrations and the latter variable causing a drawdown of nitrate concentrations. However, evidence from ^{15}N nitrification rate experiments carried out concurrently to observed *in situ* nitrate increases and tandem fluctuations in AOA *amoA* and δ^{15}N in nitrate during periods of high chlorophyll values, suggests that nitrification may fuel a significant proportion of nitrate *in situ* that is assimilated by phytoplankton. An N:P ratio that was consistently and significantly above the Redfield ratio of 16:1, also may suggest that phytoplankton were rarely nitrogen limited thereby reducing the potential importance of *in situ* N$_2$ fixation and indicating that recycling of Nr via nitrification may be a more important process fueling primary productivity in the lower CR. So, in addition to facilitating Nr flux from the CR to coastal systems, *in situ* river nitrification may fuel a significant portion of phytoplankton derived particulate organic carbon (POC), which may then be transported to coastal systems for further processing, and perhaps sequestration.

In the spatial survey of nitrification, increases in AOA *amoA* and the AOA:β-AOB *amoA* ratio were associated with high salinity, turbidity, and ammonium concentrations at bottom depths, consistent with the higher AOA abundances observed in the ocean, hypothesized particle attachment or light inhibition, and niche partitioning. These results suggest that AOA may be significant contributors to ammonia oxidation in the CRE and the CR during upwelling conditions that provide high nutrient and low

oxygen concentrations, and during low flow, high primary productivity river conditions. The results demonstrating a positive correlation between AOA:β-AOB *amoA* ratios and salinity, contrasts with some recent reports in estuaries, highlighting the need for adequate temporal resolution in estuaries as well as consideration of basic estuarine characteristics, such as residence time, upwelling events, sediment characteristics and potentially large Nr sources like estuarine turbidity maxima and lateral embayments.

4.2 Implications and Future Research

The implications of the research conducted in this thesis, supports the continued investigation of the Nr cycle in the CRS as well as further exploration of nitrification in other riverine and estuarine systems. With the year-long time series data available from SATURN-05, Nr net fluxes are now available for analysis. With similar data sets being assembled at parallel biogeochemical observatories in the CRE and the Willamette River, a more refined Nr budgeting analysis will soon be possible. To complement the time series data at these observatories and determine the contributions of nitrification and denitrification to Nr mobilization, recycling, and removal at these various sites, similar studies coupling molecular characterization of these communities with independent and temporally sensitive biogeochemical measurements are promising areas of further study. Specifically, in the case of nitrification and ammonia oxidation, better temporal and spatial resolution may shed more light as to how relatively important AOA, AOB and even heterotrophic nitrifiers are in various spatial and temporal compartments. Methodological improvements in the molecular characterization of the nitrifier community, including increased phylogenetic characterization and quantification of gene

expression are necessary in this regard. Nonetheless, it may currently be possible to reliably use the AOA:AOB ratio to determine the trophic condition of a water body as high nutrient conditions lead to high AOB/low AOA populations and low nutrient conditions lead to high AOA/low AOB populations. Studies of the relative abundance of ammonia-oxidizers may be more sensitive in this regard, when they are conducted in water columns in contrast to sediments, where high organic matter and particle load reduces the sensitivity of this proposed ecological indicator of trophic status. Also, primary production in freshwater bodies that derive most of their Nr needs from nitrification may be buffered from toxic N_2 fixing cyanobacterial blooms, as long as phosphorous loading is managed effectively.

Finally, further elucidation of the more intricate interference mechanisms of DOC on the fluorometric ammonium method should be advanced since a large and simple absorptive interference has now been identified. More simply, the IFE correction, as applied to the fluorometric determination for ammonium, should lead to increased accuracy and ease of ammonium determination in cases of high DOC concentrations.

	AOA *amoA*	β-AOB *amoA*	AOA:β-AOB *amoA* ratio	Salinity	Ammonium	Nitrate	Nitrite	Phosphorous	Silicate	Temp.	Oxygen	Chloro-phyll	Light Transm.
AOA	1.000												
β-AOB	0.085	1.000											
AOA:β-AOB	**0.908**	-0.340	1.000										
Salinity	**0.715**	-0.224	**0.769**	1.000									
Amm.	0.631	-0.048	0.615	0.676	1.000								
Nitrate	**0.799**	-0.080	**0.788**	**0.877**	0.584	1.000							
Nitrite	0.631	0.029	0.583	0.386	0.198	0.561	1.000						
Phosph.	**0.757**	0.163	0.646	0.425	0.398	0.624	0.448	1.000					
Silicate	-0.694	0.019	-0.663	-0.690	-0.519	**-0.766**	-0.333	-0.498	1.000				
Temp.	**-0.705**	0.232	**-0.763**	**-0.991**	-0.639	**-0.876**	-0.369	-0.459	0.662	1.000			
Oxygen	**-0.764**	0.215	**-0.812**	**-0.987**	-0.679	**-0.916**	-0.408	-0.506	**0.726**	**0.988**	1.000		
Chl.	**-0.799**	0.107	**-0.799**	**-0.819**	-0.641	**-0.834**	-0.397	**-0.712**	0.649	**0.840**	**0.861**	1.000	
Transm.	-0.478	-0.262	-0.341	-0.241	-0.163	-0.216	-0.263	-0.309	0.200	0.209	0.193	0.226	1.000

Table A.1 Pearson correlations between AOA *amoA* gene copies, β-AOB *amoA* gene copies, the AOA:β-AOB *amoA* gene copy ratio and environmental variables in the lower CR and CRE during July 2008. Bold indicates a significant correlation ($p < 0.05$).
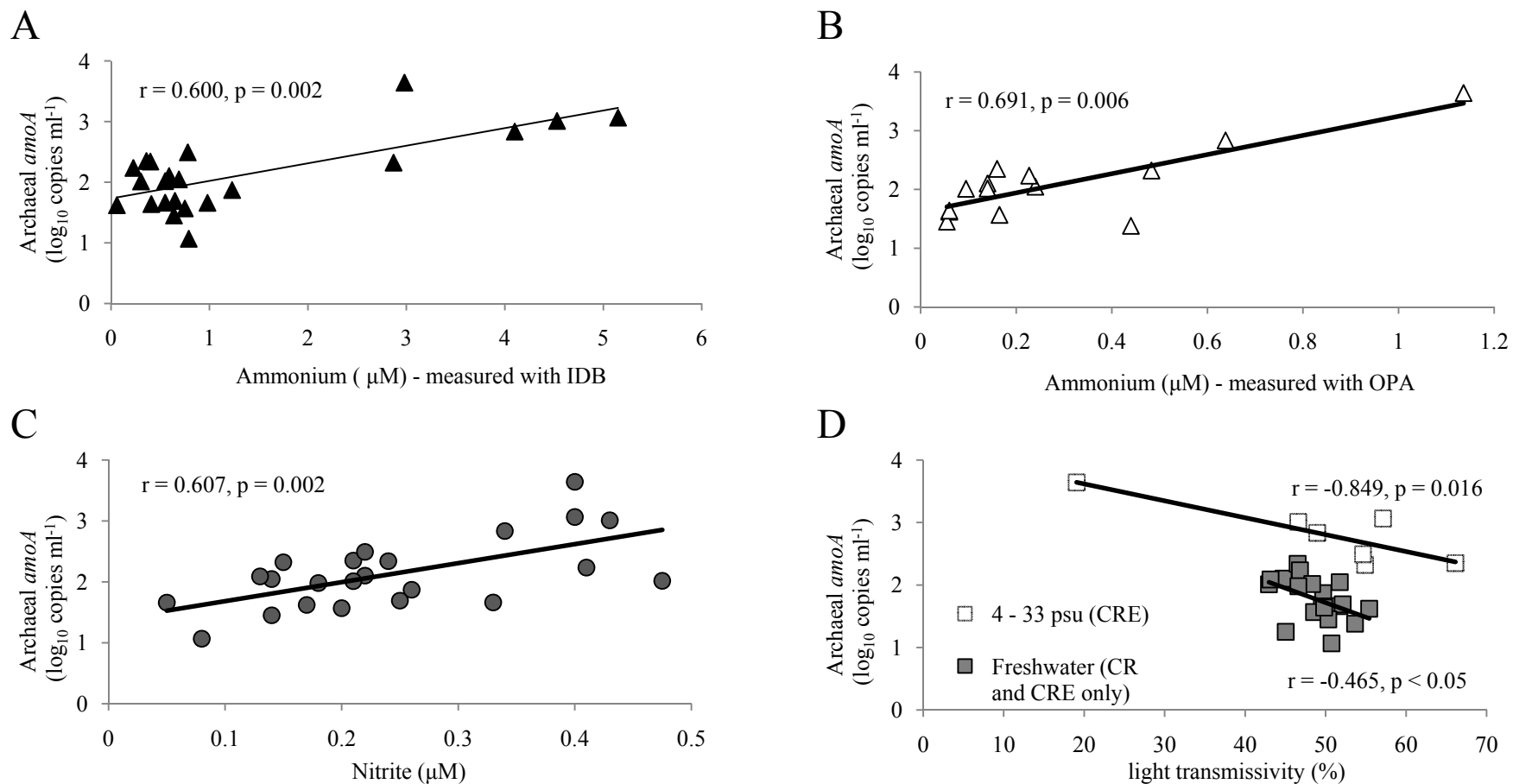
Figure A.1 Relationships between archaeal *amoA* genes and environmental variables in the lower CR and CRE. (a) and (b) depict relationships between archaeal *amoA* genes and ammonium concentrations, as measured using orthophthaldialdehyde (OPA) and indophenol blue (IDB), respectively. (c) displays the relationship between archaeal *amoA* and nitrite concentrations. (d) depicts the relationships between archaeal *amoA* genes and light transmissivity in ocean influenced bottom waters in the CRE and in freshwater samples collected only in the lower CR and CRE. Pearson correlation coefficients and p values are displayed. Error bars omitted for clarity.
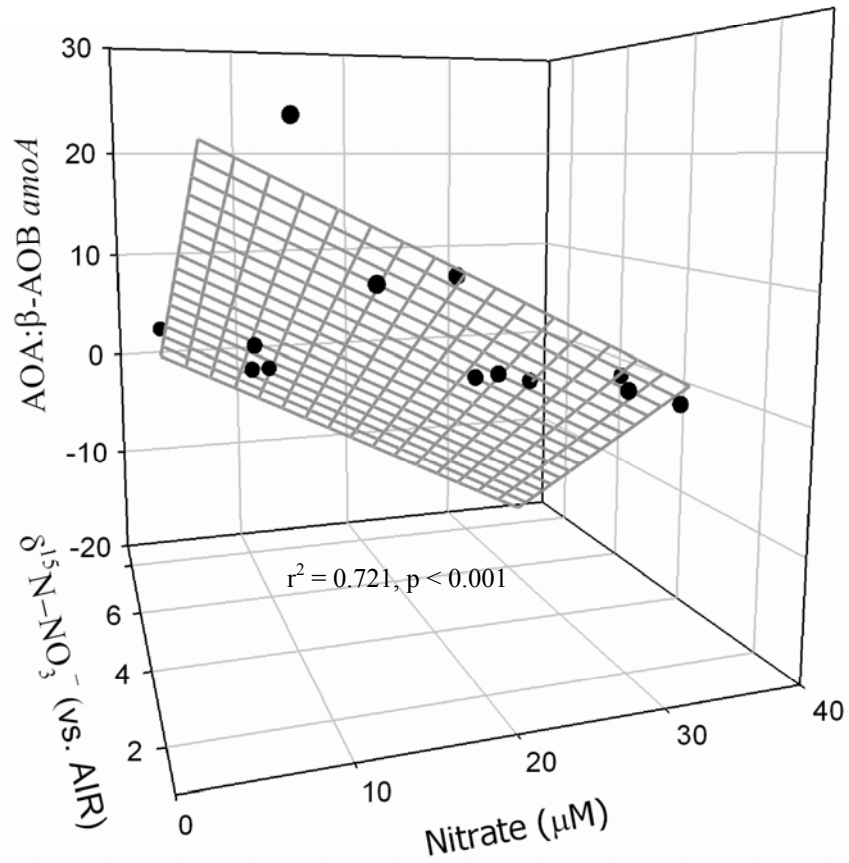
Figure A.2 3-D multiple regression plot for the relationship between the AOA:β-AOB *amoA* gene copy ratio, nitrate concentrations and $\delta^{15}N$ of nitrate, at SATURN-05. The AOA:β-AOB *amoA* gene copy ratio was found to be significantly and negatively correlated to nitrate and to the $\delta^{15}N$ of nitrate with a r^2 value of 0.721 ($p < 0.001$).
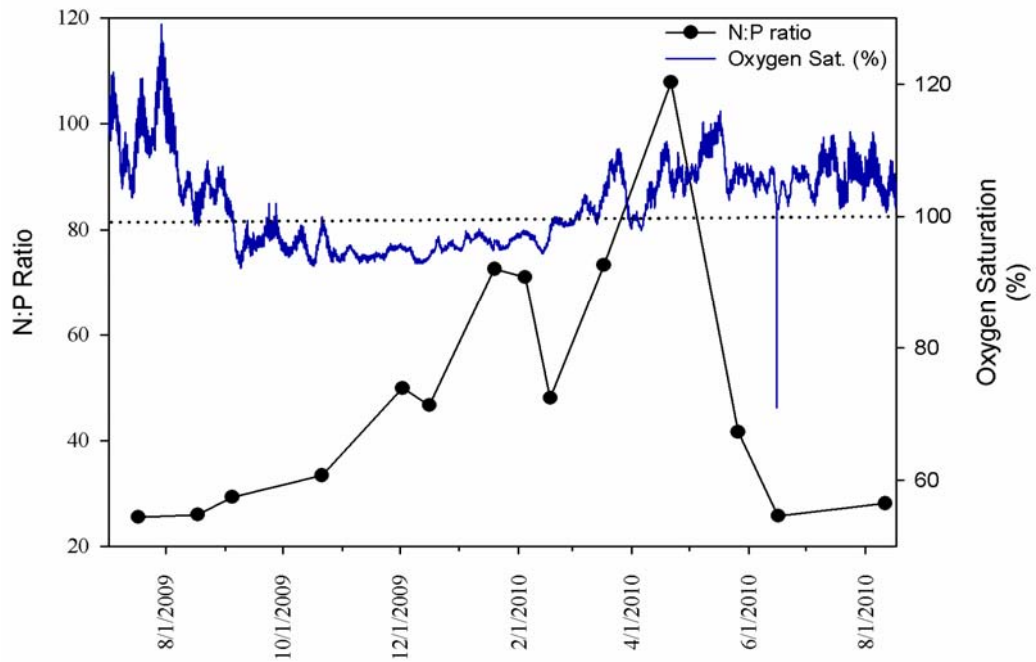
Figure A.3 Time series from July 2009 to August 2010 at SATURN-05, depicting N:P ratio in discrete black circles and oxygen percent saturation in the continuous blue line. The dotted line demarcates 100% O_2 saturation during the course of the time series.
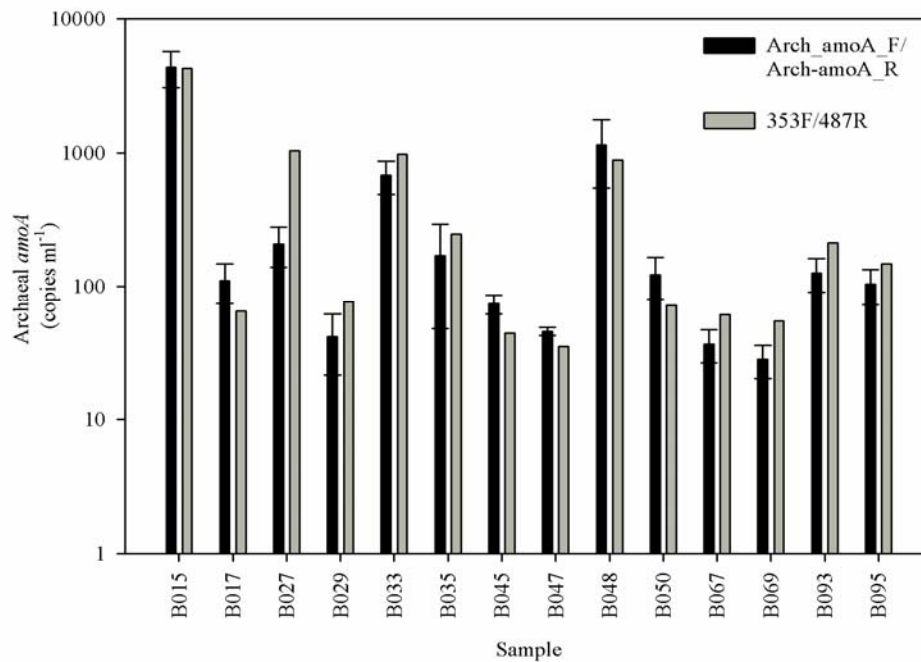
Figure A.4 Comparison of AOA *amoA* gene quantification with primer set used for the entire study (Arch_amoA_F/Arch-amoA_R) and a primer set used for a small subset of samples (353F/487R; H. M. Simon and coworkers; unpublished results). Error bars not available for 353F/487R.